

Intermittent Cauchy walks enable optimal 3D search across target shapes and sizes

M. Stromieri¹, E. Natale², A. Korman^{1*}

¹Department of Computer Science, University of Haifa, Haifa, Israel.

²CNRS and Université Côte d’Azur, Nice, France.

*Corresponding author(s). E-mail(s): amoskorman@cs.haifa.ac.il;

Abstract

Target shape, not just size, plays a pivotal role in determining detectability during random search. We analyze intermittent Lévy walks in three dimensions, and mathematically prove that the widely observed Cauchy strategy (Lévy exponent $\mu = 2$) uniquely achieves scale-invariant, near-optimal detection across a broad spectrum of target sizes and shapes. In a domain of volume n with boundary conditions, expected detection time for a convex target of surface area Δ optimally scales as n/Δ . Conversely, Lévy strategies with $\mu < 2$ are slow at detecting targets with large surface area-to-volume ratios, while those with $\mu > 2$ excel at finding large elongated shapes but degrade as targets become wider. Our results further indicate a continuous geometric transition: volume dictates detection near $\mu = 1$, ceding dominance to surface area as $\mu \rightarrow 2$, after which surface area and elongation couple to govern detection. Ultimately, 3D search introduces a pronounced sensitivity to target shape that is absent in lower dimensions. Our work provides a rigorous foundation for the Lévy flight foraging hypothesis in 3D by establishing the scale-invariant optimality of the Cauchy walk. Furthermore, our results reveal dimensionality-driven shape vulnerabilities and offer testable predictions for biological and engineered systems.

Introduction

Lévy walks consist of random movements with power-law-distributed step lengths. These patterns have been widely observed across taxa and have long been proposed as efficient strategies for locating sparse, unpredictably distributed targets [Shlesinger and Klafter \(1986\)](#); [Viswanathan et al. \(1999\)](#). Heavy-tailed displacement patterns, often with exponents near the Cauchy value $\mu = 2$, were documented in a wide range

of organisms [Harris et al. \(2012\)](#); [Ariel et al. \(2015\)](#); [Reynolds et al. \(2007\)](#); [Humphries et al. \(2010\)](#); [Sims et al. \(2008\)](#); [Boyer et al. \(2006\)](#); [Rhee et al. \(2011\)](#); [Reynolds and Frye \(2007\)](#); [Bartumeus et al. \(2003\)](#); [Raichlen et al. \(2014\)](#); [de Jager et al. \(2011\)](#). These empirical findings were linked to the Lévy flight foraging hypothesis, which posits that natural selection should favor Lévy flight movement patterns with $\mu \approx 2$, due to their presumed optimality in foraging contexts [Viswanathan et al. \(2008\)](#).

However, despite early claims of the optimality of Cauchy walks [Viswanathan et al. \(1999\)](#), the conditions under which particular Lévy exponents are advantageous remain subtle. In fact, recent results [Levernier et al. \(2020\)](#) have shown that under continuous detection, no single exponent is universally optimal in two or more dimensions, contradicting the conclusions of [Viswanathan et al. \(1999\)](#) and undermining the original theoretical basis for the Lévy flight foraging hypothesis. This raises an algorithmic question: under what conditions are Lévy motions actually advantageous?

In finite two-dimensional domains, one answer emerged in the context of intermittent search [Bénichou et al. \(2011\)](#), in which non-detecting relocation phases alternate with brief sensing phases. [Guinard and Korman \(2021\)](#) showed that when searching in 2D for rare targets of unpredictable size, intermittent Cauchy motion achieves scale-invariant, near-optimal detection performance across orders of magnitude in target size. In contrast, Lévy walks with $\mu \neq 2$ are efficient only within narrow size ranges. These results provided the first rigorous theoretical foundation for the Lévy flight foraging hypothesis in dimensions higher than one.

Here, we extend this theory to three dimensions, a setting relevant to multiple biologically realistic search domains, from marine predators seeking patches of fish [Humphries et al. \(2010\)](#); [Sims et al. \(2008\)](#) and marine microzooplankton seeking motile microalgae [Bartumeus et al. \(2003\)](#) to immune cells patrolling tissues in search of pathogens [Harris et al. \(2012\)](#). In these contexts, the “target” is a spatial subregion of elevated density, for example, a prey-rich patch or a pathogen-dense microenvironment.

To model such search scenarios, we extend the two-dimensional framework established in [Guinard and Korman \(2021\)](#) to three dimensions. We consider an intermittent Lévy searcher within a 3D cubic torus with periodic boundary conditions, a setting that effectively represents both a single target in a finite volume and an infinite, regularly spaced array of targets in an unbounded space [Viswanathan et al. \(1999\)](#); [Bénichou et al. \(2011\)](#). To evaluate performance with respect to a target S , we employ a competitive analysis approach to define the search *overhead*. This overhead is calculated as the ratio between a strategy’s mean detection time of S and the *optimal mean detection time*, that is, the theoretical minimum achievable by any strategy perfectly tuned to S . A search strategy is called *efficient* with respect to S if it incurs low overhead.

Our analysis reveals that search efficiency in three dimensions marks a fundamental departure from the 2D case. While search in two dimensions is largely governed by a single scale, namely, the target’s diameter, 3D search performance is dictated by an intricate interplay of volume, surface area, and elongation, introducing a pronounced sensitivity to target shape that is absent in lower dimensions.

						
$\mu < 2$	✓	×	×	×	×	×
$\mu = 2$	✓	✓	✓	✓	✓	✓
$\mu > 2$	×	✓	×	✓	✓	✓

Fig. 1: Search efficiency across Lévy regimes and target geometries. Summary of the performance of ballistic ($\mu < 2$), Cauchy ($\mu = 2$), and diffusive ($\mu > 2$) intermittent Lévy walks across three fundamental target geometries—balls, discs, and lines—at both small and large scales. Performance is measured relative to the optimal search strategy tuned to the specific geometry. In our rigorous proofs, efficiency (✓) indicates that the performance ratio is tight up to lower-order terms, and inefficiency (×) corresponds to a polynomial gap in system parameters. Green and Red denote efficiency and inefficiency, respectively, as established by rigorous mathematical proofs (and corroborated by simulations); Yellow indicates efficiency supported solely by numerical simulations.

Against this backdrop of highly variable, shape-dependent performance, we identify a unique property at $\mu = 2$. We mathematically prove that the Cauchy strategy serves as a “geometric equalizer”, achieving near-optimal, scale-invariant detection across a diverse spectrum of geometries, including balls, discs, and lines, even in the presence of surface irregularities. Specifically, the Cauchy strategy enables detection of convex targets in an expected time scaling as n/Δ (where n denotes the domain volume and Δ the target surface area), nearly attaining the theoretical optimum without requiring any tuning to the target. In contrast, all other Lévy strategies suffer significant efficiency losses as they encounter different geometric regimes: ballistic walks ($\mu < 2$) are penalized by small spheres as well as flat or elongated targets of any size, while diffusive walks ($\mu > 2$) degrade when encountering large spherical or disc-like targets (see Fig. 1).

Results

We consider a searcher attempting to locate a single (not necessarily connected) target within a finite three-dimensional domain, modeled as a cubic torus

$$\mathbb{T}_n = \left[-\frac{\sqrt[3]{n}}{2}, \frac{\sqrt[3]{n}}{2} \right]^3,$$

of volume n , with periodic boundary conditions.

The searcher starts from a random point of the torus and moves at constant speed according to a random walk strategy X , alternating between constant-duration pauses and ballistic steps whose lengths ℓ follow a prescribed distribution p in uniform directions. For $\mu \in (1, 3]$, the distribution of the (truncated) Lévy walk X^μ (see details in

Methods Section 2) is:

$$p(\ell) \sim \frac{1}{\ell^\mu}, \quad \ell \leq \frac{\sqrt[3]{n}}{2}.$$

The searcher possesses a detection radius $d \geq 1$; in detection mode, it successfully detects a given set of points if it is located within distance d of them. Hereafter, we define this entire detectable region—the collection of points within distance d of the desired set—as the target, denoted S (see Fig. 2a and Methods, Section 2). We focus on *intermittent search* Bénichou et al. (2011), where detection is only possible during the short pauses between steps, and not while moving during a step. Thus, detection occurs if, at the end of a ballistic step, the searcher is located inside S (see Fig. 2a).

The *detection time* of process X with respect to S , denoted $t_{\text{detect}}^X(S)$, is the expected time until X first detects S , averaged over the randomness of both the process X and the initial position of the searcher.

For a given target S , let X^* denote the optimal strategy, that is, the one that minimizes detection time of S . The *overhead* of a strategy X with respect to S is defined as the ratio between its detection time $t_{\text{detect}}^X(S)$ and the optimal detection time $t_{\text{detect}}^{X^*}(S)$. Consequently, efficiency is considered degraded (or increased) if this overhead increases (or decreases). In our mathematical framework, a search strategy is classified as efficient with respect to a target if its overhead is at most poly-logarithmic in the system size n . Conversely, a strategy is called inefficient if the overhead scales polynomially with n .

Geometric Framework

Our analysis suggests that the influence of target shape on search efficiency is substantially more complex in three dimensions than in two. While diameter serves as a natural size descriptor in 2D settings Guinard and Korman (2021), we were unable to identify a single geometric parameter that reliably captures optimal detection across the diverse range of 3D target shapes. Nevertheless, surface area, and related geometric variants, emerge as effective predictors of optimal search time across a broad class of shapes, particularly those that are not highly folded.

Furthermore, different Lévy exponents are sensitive to distinct geometric features. Intuitively, a Lévy walk with $\mu \approx 1$ samples the torus almost uniformly in each step; this makes the target’s volume the primary determinant of detection time. Conversely, for $\mu \approx 3$, the walk resembles Brownian motion. Because steps are small and local, the walker cannot ‘jump’ into the target’s interior but must instead intercept its boundary. Hence, detection time is fundamentally driven by boundary crossing, making surface area a natural candidate for governing detection performance. As we will demonstrate later, this intuition is insufficient to encompass the full complexity of geometric sensitivity, e.g., the observation that Brownian-like walkers detect elongated targets significantly faster than spherical ones of equivalent surface area.

Combining mathematical analysis with simulations, we demonstrate that geometric sensitivity shifts continuously with the Lévy exponent: volume dominates detection time for $\mu \approx 1$, gradually yielding to surface area, which becomes the sole governing factor at the critical point $\mu = 2$. Beyond this point, for $\mu > 2$, performance becomes sensitive to both surface area and elongation.

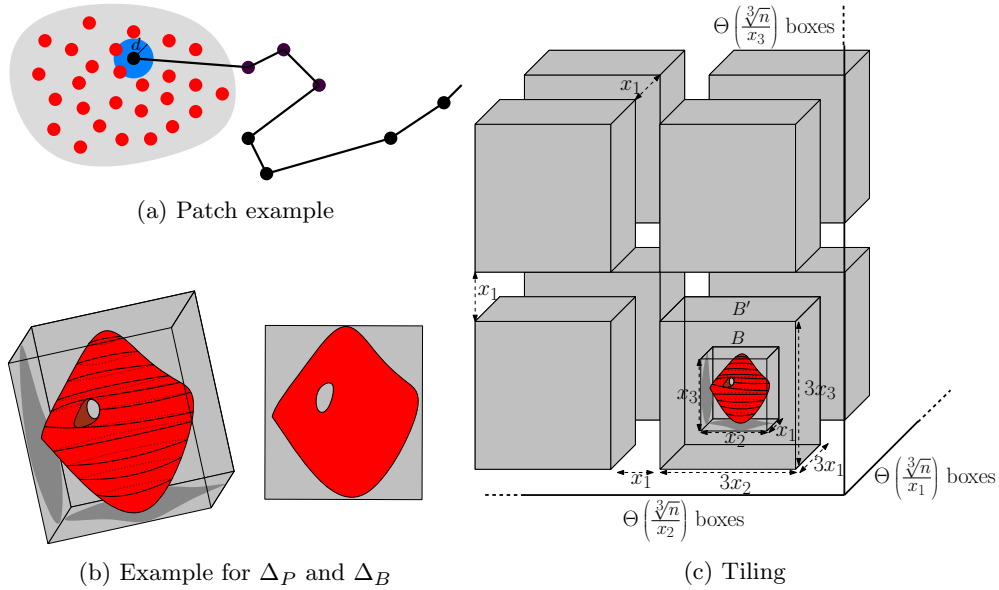
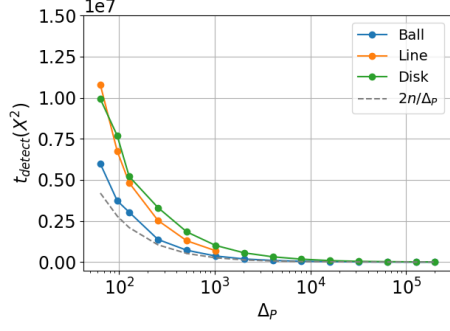


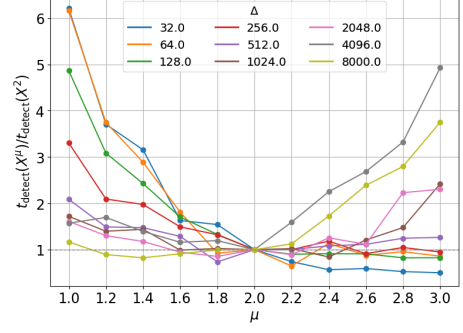
Fig. 2: Intermittent search, Bounding box, and Universal lower bound construction. Fig. 2a provides a visualization of an agent performing an intermittent Lévy walk (for simplicity of presentation, it is two-dimensional). The points to be detected (e.g., food patches) are represented by red circles, and the surrounding grey area indicates the detectable region, which we refer to as the target S ; similarly, the blue area around the searcher represents its own detection radius. In this specific instance, the agent successfully detects the prey via this range. Notably, because the search is intermittent, the agent cannot detect targets while in transit; detection occurs only upon stopping at the locations indicated by the black dots. Fig. 2b shows a target (red shape on the left) together with its minimum surface area bounding box $B = \text{Box}(S)$ (grey box on the left), which is not necessarily axis-aligned. The panel on the right illustrates the projection of the shape onto the largest face of the box; In this example, Δ_P equals the red area, while Δ_B equals the red area plus the grey area. Figure 2c depicts the tiling argument used to derive the universal lower bound in Eq. (1). For clarity, the boxes are shown as axis-aligned; in the general case, however, they need not be aligned with the coordinate axes.

The following definitions will be used to formally relate target morphology to search efficiency. Given a target S , let $\text{Box}(S)$ denote the smallest 3D box containing S .

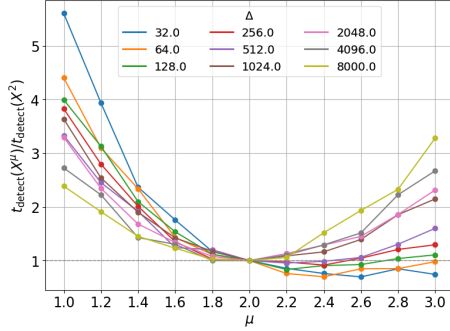
- **Largest face area (Δ_B):** This is defined as the surface area of the largest face of $\text{Box}(S)$ (Fig. 2b, left side).
- **Projected surface area (Δ_P):** This is defined by considering the orthogonal projections of S onto each of the six faces of $\text{Box}(S)$, and taking the largest surface area among these six projections (Fig. 2b, right side).



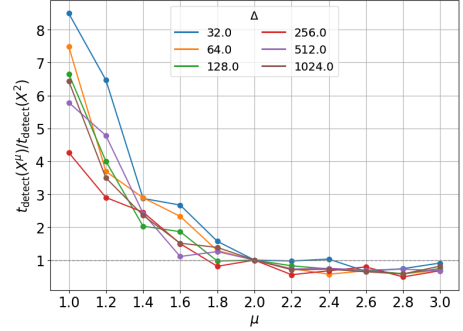
(a) Cauchy searching different shapes



(b) Relative detection time (Ball)



(c) Relative detection time (Disk)



(d) Relative detection time (Line)

Fig. 3: Comparing the detection times of different Lévy walks. All simulations correspond to the 3D torus \mathbb{T}_n with volume $n = 512^3$. Fig. 3a presents a comparison of the detection times of the Cauchy walk for *Line*, *Disk*, and *Ball* targets, all sharing the same projected surface area Δ_P , alongside the corresponding universal lower bound (dashed line). Fig. 3b displays detection-time ratios normalized by the detection time of the Cauchy walk ($\mu = 2$) for ball-shaped targets with surface area Δ (color-coded), emphasizing the relative performance of different exponents. Figs. 3c and 3d display analogous results for a disk and line-shaped targets, using the same experimental setup. Takeaway: $\mu = 2$ stays near baseline across geometries; $\mu \neq 2$ exhibits geometry-dependent slowdowns.

Note that $\Delta_B \geq \Delta_P$ for every shape S . A shape is called *approximately convex* if $\Delta_P \geq \Delta_B/36$. The choice of the factor $1/36$ allows this family to contain all convex shapes (e.g., spheres, ellipsoids, discs, cylinders), possibly with small surface irregularities such as holes or bumps, see proof in SM, Section 6.

Let x_1, x_2, x_3 denote the side dimensions of the bounding box $B = \text{Box}(S)$, where, without loss of generality, $x_1 \leq x_2 \leq x_3$. We refer to these quantities as the target's *thickness*, *width*, and *length*, respectively. Note that the target's length satisfies $x_3 = \Delta_B^\delta$, for some $\delta \in [\frac{1}{2}, 1]$, which we refer to as the *elongation* of S . For example, $\delta \approx \frac{1}{2}$

for a ball-shaped or disc-shaped target, while $\delta \approx 1$ for a long line-shaped target (see details in Section 4.3).

Universal lower bound

We proved mathematically (SM, Section 3) that, regardless of the search strategy, the detection time of S is always at least

$$\Omega\left(\frac{n}{\Delta_B}\right). \tag{1}$$

We refer to this bound as a *universal lower bound*, since it holds for any search strategy, and thus applies in particular to all Lévy walks.

To provide geometric intuition for the derivation of Eq. (1), note that the volume of the bounding box $B = \text{Box}(S)$ is given by $V = x_1x_2x_3$, and the largest face area is $\Delta_B = x_2x_3$. Analogously, define an enlarged box B' with sides $3x_1, 3x_2, 3x_3$ and volume $V' = \Theta(V)$. Consider $\Omega(n/V') = \Omega(n/V)$ different placements of B' in the torus, so that every two displacements are of distance at least x_1 apart (see Fig. 2c). Before the search starts, instead of choosing the starting point of the searcher at random, we fix it at the origin and choose the position of S randomly in the torus. With constant probability, S is fully contained in one box B' , and all such boxes have equal probability to contain it. To find S , the searcher needs to visit at least half of these box-displacements on average, and since each new visit takes at least x_1 time (the minimal distance between displacements), the total expected time is at least $\Omega(nx_1/V) = \Omega(n/x_2x_3) = \Omega(n/\Delta_B)$. This establishes Eq. (1).

Next, we seek to identify whether any intermittent Lévy walk strategy can detect S in time approaching the universal lower bound. Our analysis of the interplay between target shape and the exponent μ reveals a phase transition at $\mu = 2$.

Ballistic regime ($\mu < 2$) is penalized by targets with a large surface to volume ratio

Consider a Lévy walk with exponent $\mu \in (1, 2)$ and a target S of volume V . Let $\varepsilon = 2 - \mu$ denote the ‘distance’ from the Cauchy exponent. We first proved (SM, Section 4.1.1) a general lower bound of $\Omega(n/V)$ for the expected number of steps before finding the target, which holds for any intermittent Lévy walk. Applying a variant of Wald’s identity (SM, Claim 2.1), we can transform this lower bound into one for the detection time by scaling it by the average step length of the Lévy process. In the regime $\mu \in (1, 2)$, the mean step length is $\Theta(n^{\varepsilon/3})$ (SM, Eq. (6)), leading to the following lower bound on the detection time:

$$t_{\text{detect}}^{X^\mu}(S) = \Omega\left(\frac{n^{1+\varepsilon/3}}{V}\right). \tag{2}$$

Consider a target S whose volume V is proportional to its largest face area Δ_B . For example, a ball of constant diameter, a disc of an arbitrary diameter, or a line of arbitrary length (see Methods, Section 2). For such a target, Eq. (2) implies that

detection time is a factor of $\Omega(n^{\varepsilon/3})$ slower than the universal lower bound. This gap widens as μ decreases further from 2, with the deterioration driven by the polynomial degree $\varepsilon/3$. Due to Eq. (3) (discussed later), detection times for such targets are slower than the ones of the Cauchy walk by the same polynomial factor, up to a lower order term. Since the optimal strategy finds S at least as fast as Cauchy, the overhead (defined w.r.t the optimal strategy) is polynomial in n .

These theoretical results are consistent with our numerical simulations. Fig. 3b shows the detection time as a function of the Lévy exponent μ for ball-shaped targets of varying surface areas Δ , normalized by the detection time of the Cauchy walk ($\mu = 2$) for each corresponding Δ . In the regime $\mu < 2$, small ball targets are found more slowly by such Lévy processes than by the Cauchy searcher. Figs. 3c and 3d further show that when $\mu < 2$, detection time of disc-targets (Fig. 3c) as well as line-targets (Fig. 3d), increases as μ decreases, regardless of the target sizes. Finally, Fig. 3b suggests that large-scale balls are detected efficiently in the ballistic regime ($\mu < 2$). This performance may be attributed to the diminishing surface area to volume ratio as the radius of the ball increases.

These results indicate that increasingly ballistic strategies become less effective at detecting targets with a large surface area to volume ratio, regardless of their size, and confirm that the transition from ballistic to diffusive search at $\mu = 2$ is critical for efficient detection of such geometries.

Localized exploitation ($\mu > 2$) is penalized for large spherical and large disc-like geometries

Next, we examined Lévy walks in the diffusive regime, $\mu \in (2, 3]$. We prove that the overhead for spherical or disc-like targets is at least a polynomial factor $\Omega(\Delta^{\frac{\mu-2}{2}})$, where the penalty exponent increases as μ deviates from 2.

Specifically, we proved (SM, Corollary 4.7) that detection time of a Lévy walk X^μ with $\mu \in (2, 3]$ with respect to a ball (or a disc) target S of surface area Δ obeys the following asymptotic lower bounds:

$$t_{detect}^{X^\mu}(S) = \begin{cases} \Omega\left(n\Delta^{\frac{\mu-2}{2}-1}\right) & \text{if } \mu \in (2, 3) \\ \Omega\left(\frac{n}{\Delta^{1/2} \log \Delta}\right) & \text{if } \mu = 3 \end{cases} .$$

These lower bounds are based on a tiling argument analogous to the one used in the proof of the universal lower bound (see Fig. 2c), combined with a more nuanced lower bound on the time needed to move between boxes. Specifically, in the diffusive regime ($\mu > 2$), traversing a distance ℓ takes polynomial time in ℓ , where the exponent of the polynomial is $\mu - 1$ (SM, Claim 4.5).

Observe that in this regime of μ , detection time for a ball or a disc target with surface area Δ is larger than the universal lower bound by a polynomial factor in Δ , specifically $\Delta^{\frac{\mu-2}{2}}$. For large targets, such that Δ is polynomial in n , this factor is also polynomial in n . Due to Eq. (3) (discussed later), the detection time of the Lévy process is also slower than the Cauchy walk by the same polynomial factor, up

to the poly-logarithmic factor in n associated with the Cauchy walk. This implies a polynomial in n overhead with respect to such targets.

These theoretical findings are corroborated by our numerical simulations, which demonstrate that for spherical (Fig. 3b) and disc-like (Fig. 3c) targets, the search efficiency of diffusive strategies ($\mu > 2$) relative to the Cauchy strategy decreases as either the exponent μ or the target’s surface area increases.

These results indicate that overly localized strategies suffer from reduced efficiency with respect to large spherical and disc-like targets, reinforcing the conclusion that the transition from diffusive to ballistic search at $\mu = 2$ is critical for the efficient detection of such targets.

Scale-invariance optimality of the Cauchy Walk

Intermittency renders long relocations “blind”, meaning detection relies entirely on where the step stops. To have any chance of hitting the target, an intermittent searcher must first select a winning direction; the probability of choosing this “good angle” is dictated strictly by the target’s 2D silhouette rather than its total surface area, as a blind trajectory simply bypasses internal folds. Consequently, the success of a relocation is controlled by the target’s cross-sectional exposure along the approach vector. This highlights the projected surface area Δ_P parameter, which acts as a proxy for the maximal target area that can be “observed” across all possible viewing directions.

We proved (SM, Theorem 5.4) that for any (not necessarily connected) target S with projected surface area Δ_P , the detection time of the Cauchy walk X^{cauchy} satisfies:

$$t_{\text{detect}}^{X^{\text{cauchy}}}(S) = \mathcal{O}\left(\frac{n \log^3 n}{\Delta_P}\right). \quad (3)$$

Informally, the proof of Eq. (3) (see SM, Section 5) uses the projected surface area $\Delta_P(S)$ to identify a subset of S whose properties render its hitting time more analytically tractable. More specifically, leveraging the geometrical properties of the projection S onto the bounding box, the proof constructs a subset $S^* \subseteq S$ which consists of $\Theta(\Delta_P)$ balls of radius 1, with the property that within any given ball of radius $r > 1$, there are at most $\mathcal{O}(r^2)$ such balls. These properties are particularly helpful for upper-bounding the expected number of returns to S^* , a key step in establishing an upper bound on the hitting time of S^* . Since $S^* \subseteq S$, this upper bound also serves as an upper bound on the hitting time of S .

Recall that the largest face area Δ_B and the projected surface area Δ_P of an approximately convex target are proportional. Combined with Eqs. (1) and (3), this implies that a Cauchy walk finds such a target in optimal time, up to a poly-logarithmic factor in n . In particular, for a convex target with surface area Δ , the detection time is at most the optimal bound of n/Δ , times a poly-logarithmic factor in n .

We further showed (SM, Section 6.3) that, unlike the convex case, for arbitrary shapes, the projected surface area Δ_P in Eq. (3) cannot be replaced by either the target’s surface area Δ or the largest face surface area Δ_B .

Simulation results support our asymptotic mathematical findings. Fig. 3a depicts the detection times of the Cauchy walk on the torus for both lines, discs, and balls, with equal projected surface area Δ_P (see Methods, Section 2). These plots demonstrate that Cauchy’s detection time is proportional to the universal lower bound, suggesting that the poly-logarithmic factor predicted by Eq. (3) is negligible in practice.

Figs. 3b, 3c and 3d demonstrate the overall superiority of the Cauchy walk as a robust, geometry-agnostic search strategy. While searchers in the exploration-dominated ($\mu < 2$) or exploitation-dominated ($\mu > 2$) regimes perform well for specific target scales and shapes, they suffer substantial efficiency losses when faced with mismatched target sizes and geometries. In contrast, the Cauchy walk ($\mu = 2$) identifies a critical point of geometric invariance, maintaining near-optimal detection times across a spectrum of target geometries: from spheres (Fig. 3b) and flat discs (Fig. 3c) to highly elongated targets (Fig. 3d).

Different Lévy walks are sensitive to different geometrical properties

Integrating mathematical analysis with numerical simulations, we show that geometric sensitivity evolves continuously with the Lévy exponent: while volume dictates detection time in the ballistic regime ($\mu \approx 1$), it gradually cedes dominance to surface area, which emerges as the primary governing parameter at the critical point $\mu = 2$. Conversely, in the diffusive regime ($\mu > 2$), detection performance becomes multifaceted, determined by a coupling of surface area and target elongation.

Consider first a Lévy walker in the regime $\mu \in (1, 2)$. Eq. (2) provides a lower bound on its detection time concerning any target S with volume V . Recall that this lower bound is composed of a lower bound on the number of steps m before finding S , namely, $\Omega(\frac{n}{V})$, times the average step length, which is $\Theta(n^{\varepsilon/3})$, where $\varepsilon = 2 - \mu$. For $\mu \approx 1$, the process is close to sampling the torus uniformly in each step, implying that the number of steps m scales like n/V . Together, these bounds yield a tight bound of $\Theta(\frac{n^{1+\varepsilon/3}}{V})$ for the detection time, highlighting volume as the target’s critical geometric parameter, governing detection time in scenarios where $\mu \approx 1$.

Fig. 4a illustrates the detection time ratio between a ball and a line of equivalent volume, for different exponents μ . The relatively flat profiles observed for $\mu \leq 1.4$ suggest that, in this regime, detection is primarily volume-driven. Furthermore, Fig. 4b presents the ratio of detection times for a ball and a line with equal surface area Δ . Here, the dashed line represents the volume ratio of the two targets; the proximity of the plots to this line at small μ values further supports volume as a dominant geometric parameter in this regime. Moreover, Figs. 4a and 4b demonstrate a relatively smooth transition from volume to surface area, where the latter is represented by the dashed line in Fig. 4a, and the horizontal line $y = 1$ in Fig. 4b.

For the Cauchy walk ($\mu = 2$), Eq. (3) shows that the detection time of a convex target with surface area Δ scales like the universal lower bound n/Δ , up to a poly-logarithmic factor in n . This highlights surface area as the critical geometric parameter governing optimal detection time, and, in particular, the most relevant geometric parameter for the case $\mu = 2$. Accordingly, as predicted by combining Eqs. (1) and (3), Fig. 3a demonstrates that despite the substantial difference in volume between the

corresponding line, disk, and ball shapes, their detection times by the Cauchy walk remain comparable due to their projected surface area similarity.

Next, we considered Lévy walks with exponent $\mu \in (2, 3]$, and showed that the detection time is strongly affected by both surface area and elongation. Indeed, these searchers are exceptionally efficient at locating highly elongated targets; however, their performance degrades rapidly as the target becomes wider, that is, as the second-largest dimension of the bounding box, increases.

Specifically, we proved (SM, Theorem 4.6) that detection time of a target S with elongation δ obeys the following asymptotic lower bounds:

$$t_{\text{detect}}^{\chi^\mu}(S) = \begin{cases} \Omega\left(n\Delta_B^{\varepsilon(1-\delta)-1}\right), & \text{if } \mu = 2 + \varepsilon, \text{ with } 0 < \varepsilon < 1, \\ \Omega\left(\frac{n}{\Delta_B^\delta \log \Delta_B}\right), & \text{if } \mu = 3. \end{cases} \quad (4)$$

In this regime of μ , detection time for approximately convex targets with a largest face area of Δ_B (or equivalently, a projected surface area) is slower than the Cauchy walk by a polynomial factor Δ_B^c , where $c = \varepsilon(1 - \delta)$, up to a poly-logarithmic factor in n . The exponent c scales positively with μ and inversely with δ .

While the lower bounds defined in Eq. (4) are maximized for ball or disc shapes ($\delta = 1/2$), they become closer to the universal lower bound of $\Omega(n/\Delta_B)$ as the elongation parameter δ approaches 1. Consistent with this, Fig. 4d illustrates how detection time of rectangles (see definition in Methods, Section 2) increases as δ decreases (i.e., the target becomes wider), while maintaining the same surface area.

Next, we demonstrate that elongated targets are located with high efficiency by Lévy searchers in the diffusive regime ($2 < \mu \leq 3$). We provide analytical evidence by analyzing a discretized version of the process (see Methods, Section 2), proving that the detection time for a line target of length L is $O((n/L) \log n)$ (see SM, Section 7). For the discrete grid, it is easy to adjust the argument behind the universal lower bound (Eq. (1)) to obtain an $\Omega(n/L)$ lower bound for the detection time of the line. Hence, such Lévy walks incur only a logarithmic overhead. As $n \rightarrow \infty$, this discrete approximation can be expected to converge to the continuous domain setting with detection radius being 1, suggesting that these scaling results hold also for the continuous setting.

The proof is based on the following intuition. Assume the target is a line of length L , oriented parallel to the x -axis. Consider the Lévy walk projected onto the yz -plane, and let v be the point representing the projection of the target line onto this plane. This projected process behaves as a Lévy walk with the same exponent on a 2D domain of area $n^{2/3}$; consequently, the expected time for the projected walk to hit v is $\mathcal{T} := \mathcal{O}(n^{2/3} \log n)$ (SM, Theorem 7.2). At the moment of impact with v , the 3D walk is effectively mixed on the 3D torus (SM, Theorem 7.9), implying that all points along the line segment orthogonal to v (which contains the target and has a total length of $n^{1/3}$) are roughly equally likely to be occupied by the walker. This yields a conditional detection probability of $\Theta(L/n^{1/3})$. Hence, by time \mathcal{T} , detection occurs with probability $p := \Theta(L/n^{1/3})$. Summing these independent geometric trials yields a total expected detection time of $\mathcal{T}/p = \mathcal{O}((n/L) \log n)$. Accordingly, our simulations

(Fig. 3d) confirm that this accelerated detection of line targets is comparable to that of the Cauchy walk, and remains robust across this entire diffusive range.

Finally, consistent with the lower bounds in Eq.(4), Figs. 4a and 4b demonstrate that long lines are detected significantly faster than balls of equal volume (Fig. 4a) or surface area (Fig. 4b). This indicates that surface area, while dominant at $\mu = 2$, is no longer a sufficient descriptor once μ enters the diffusive regime.

These results suggest that, in addition to the surface area, elongation plays a critical role for the detection time in the diffusive regime $\mu \in (2, 3]$.

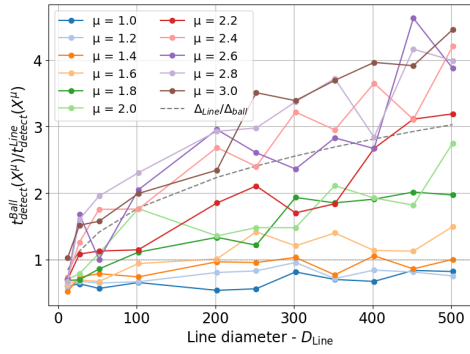
Discussion

Lévy walks are among the most extensively studied models of animal movement, yet debate persists over the conditions under which they yield optimal search performance [Viswanathan et al. \(1999\)](#); [Bénichou et al. \(2011\)](#); [James et al. \(2011\)](#); [Levernier et al. \(2020\)](#). Here, we advance the mathematical theory of intermittent Lévy search from two to three dimensions, a biologically relevant setting that reflects the environments of diverse search processes, from marine predators [Humphries et al. \(2010\)](#); [Sims et al. \(2008\)](#) to immune cells [Harris et al. \(2012\)](#).

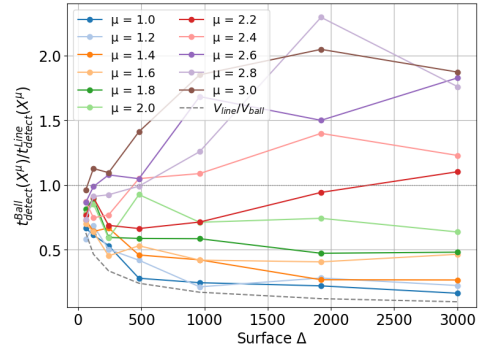
Our results establish the Cauchy strategy ($\mu = 2$) as a uniquely robust intermittent strategy for navigating unpredictable 3D environments. We provide a mathematical proof that $\mu = 2$ achieves near-optimal, scale-invariant detection across a diverse spectrum of target scales and convex morphologies. This performance is characterized by a remarkable stability: while specialized Lévy exponents may offer marginal gains for specific target geometries, the Cauchy strategy remains near-optimal without parameter tuning, matching the theoretical bound even as target dimensions vary by multiple orders of magnitude. By consistently mirroring the peak performance of specialized strategies across all scenarios, the Cauchy strategy provides a universal search solution that effectively resolves the fundamental trade-off between localized exploitation and global exploration.

Our findings reveal that beyond size, target geometry exerts a profound influence on the detection efficiency of a given Lévy strategy, with these effects varying significantly across the Lévy spectrum. For example, exploration-dominated searchers ($\mu < 2$) detect large spherical targets efficiently but are markedly slow at locating elongated targets. Conversely, exploitation-dominated searchers ($\mu > 2$) excel at identifying line targets but struggle to detect large spheres. Notably, both regimes ($\mu \neq 2$) exhibit diminished performance when searching for large discs.

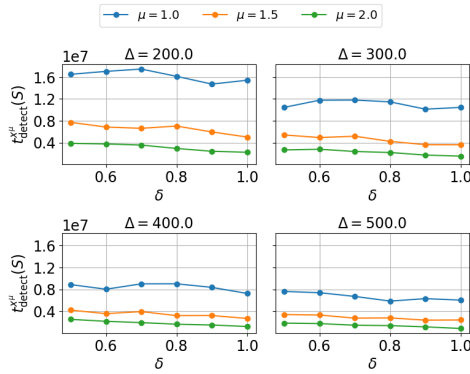
We further demonstrate a transition in geometric sensitivity as the Lévy exponent varies. To illustrate the sensitivity of these search regimes, consider a target of fixed volume V seeking to maximize its surface area while remaining convex. One could stretch this volume into a line of length $L \approx V$, or alternatively, into a thin disc of radius $R \approx \sqrt{V}$. Aiming to evade a Lévy searcher in the regime $\mu > 2$, the choice of geometry is critical: the disc-like configuration is much harder to detect than the line, offering a significant survival advantage. However, this “geometric sanctuary” disappears under the Cauchy strategy ($\mu = 2$), which demonstrates comparable effectiveness in detecting both targets, as they share a similar surface area.



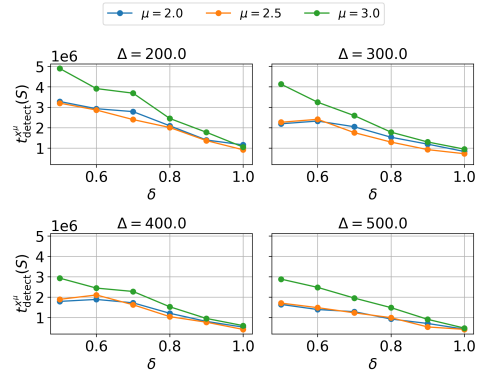
(a) Detection time ratio with fixed volume



(b) Detection time ratio with fixed surface area



(c) Varying δ , $\mu \in \{1, 1.5, 2\}$



(d) Varying δ , $\mu \in \{2, 2.5, 3\}$

Fig. 4: Detection-time phase transition induced by varying μ and dependency on elongation. All simulations are performed on a three-dimensional torus \mathbb{T}_n with volume $n = 512^3$. Fig. 4a shows the ratio of detection times for a ball and a line of equal volume, for several values of μ . The x -axis corresponds to the line length D_{Line} , while the diameter of the corresponding ball is chosen so that the two volumes are equal. The dashed grey line shows the ratio of the surfaces of the two targets, representing a theoretical estimation for the detection time ratio of the Cauchy walk. Similarly, Fig. 4b presents the ratio of detection times for a ball and a line with the same surface area Δ , shown on the x -axis. In this figure, the dashed line represents the ratio of the volumes of the two targets, serving as a theoretical estimation for the Lévy walk as $\mu \rightarrow 1$. Fig. 4c presents detection times for Lévy walks with $\mu \in \{1, 1.5, 2\}$, where the targets are rectangles with side lengths Δ^δ and $\Delta^{1-\delta}$. Similarly, Fig. 4d shows the result for the same set of experiments when $\mu \in \{2, 2.5, 3\}$. Takeaway: the governing geometric control shifts from volume to surface, and then to surface and elongation as μ increases.

Moreover, this reveals a dimensionality-induced reversal in search vulnerability. In 2D, large targets, including elongated ones, enjoy a form of “protection” against exploitation-dominated strategies ($\mu > 2$), which detect them significantly more slowly than the Cauchy walk [Guinard and Korman \(2021\)](#). In 3D, however, this protection collapses specifically for elongated shapes, as they become highly vulnerable across the entire spectrum of $\mu \geq 2$. This suggests that ecological niches in 3D dominated by diffusive searchers impose more aggressive selective pressures on prey morphology, favoring spherical shapes over elongated ones.

Our theoretical bounds further sharpen this picture by showing that for approximately convex targets, the optimal detection time is tightly governed by the projected surface area. While non-convex regimes, such as the highly folded structures of DNA, present additional complexities, our results suggest that the projected surface area remains an informative descriptor of detectability.

While our mathematical framework provides a robust theoretical baseline for 3D intermittent search, biological search is inherently complex. In particular, our model abstracts away continuous sensory tracking, prey mobility, and environmental clutter. Nevertheless, for species governed by intermittent mechanics, our geometric perspective yields highly testable evolutionary predictions. We predict that “generalist” 3D intermittent foragers will exhibit a strong evolutionary convergence toward Cauchy-like ($\mu \approx 2$) flight patterns to remain robust against highly variable prey morphologies. Conversely, species specializing in specific target geometries should predictably deviate from this universal optimum—for instance, evolving $\mu > 2$ strategies when hunting predominantly elongated prey, or $\mu < 2$ regimes for dense, voluminous swarms.

Together, our results provide a unified framework linking movement statistics, geometry, and efficiency. By establishing the singular scale and shape invariance optimality of the Cauchy walk in 3D, we provide a rigorous theoretical foundation for the Lévy flight foraging hypothesis [Viswanathan et al. \(2008\)](#). Ultimately, our work suggests that the coevolution of search strategy and target morphology is a fundamental principle of spatial ecology, with wide-ranging applications from marine biology to the design of autonomous robotic swarms.

Methods

Model

The torus \mathbb{T}_n is identified with the cubic domain $[-\sqrt[3]{n}/2, \sqrt[3]{n}/2]^3$ of volume n , embedded in the Euclidean space \mathbb{R}^3 , with periodic boundary conditions, that is, opposite faces of the cube are identified. Let $\mu \in (1, 3]$ and $\ell_{\max} > 1$ denote the maximal admissible step length (possibly $\ell_{\max} = \infty$). A *Lévy walk* Z^μ on \mathbb{R}^3 (or X^μ on \mathbb{T}_n) with maximal step length ℓ_{\max} is defined as a random walk process whose step lengths are distributed according to:

$$p(\ell) = \begin{cases} a, & \text{if } \ell \leq 1, \\ a\ell^{-\mu}, & \text{if } 1 < \ell < \ell_{\max}, \\ 0, & \text{if } \ell \geq \ell_{\max}, \end{cases} \quad (5)$$

where the normalization constant

$$a = \left(1 + \int_1^{\ell_{\max}} \ell^{-\mu} d\ell \right)^{-1}$$

ensures that $\int_0^\infty p(\ell) d\ell = 1$. When the process is confined to the torus \mathbb{T}_n , we set $\ell_{\max} = \sqrt[3]{n}/2$. In the special case where $\mu = 2$, the corresponding process is referred to as a *Cauchy walk*, and its realization on the torus is denoted by X^{cauchy} .

The search process starts at a random location of the torus, chosen uniformly at random. In each step m of the Lévy walk, the process chooses a direction uniformly at random, and a step length ℓ according to the distribution $p(\ell)$. The result is a vector $V(m)$, called *relocation* vector. The process then moves over the torus from its current position $X(m-1)$ to $X(m) = X(m-1) + V(m)$, modulo the torus, i.e., respecting its boundary conditions.

The *detection radius* of the searcher is $d \geq 1$.

We consider a subset of points S' in the torus, called the *raw target*, which may be connected or consist of several disjoint components. For the purpose of our analysis, we define the detectable region $S \subset \mathbb{T}_n$ as the set of all points within the detection radius d of some point in S' . We hereafter use the term target to refer to this detectable region S , rather than the raw target S' . Throughout, we assume that the target's volume is well defined, and that its surface is piecewise smooth so that its surface area, as well as the surface area of its projections onto planes, are well defined. We further note that all our results concerning different parameters of the target, e.g., its surface area, correspond to S and not to the raw target S' .

We focus on *intermittent search*, where it is assumed that the target S cannot be detected while the agent is in motion, that is, during a transition from $X(m)$ to $X(m+1)$. In this setting, the target is detected at step m if the agent's position at the end of the step satisfies $X(m) \in S$.

Geometric objects

We considered four types of raw target geometries: disks, balls, lines, and rectangles. Recall that because of the detection radius $d \geq 1$, the searcher effectively spots the target by interacting with its *detectable region*. As a consequence, a disk target is thickened into a region of total thickness $2d$, while a *line* target of length L is expanded into a cylinder-like region of length $L + 2d$ and diameter (or width) $2d$. Similarly, rectangles are 2D rectangular objects extruded with thickness equal to the detection radius d in the third dimension.

A shape is called *approximately convex* if $\Delta_P \geq \frac{1}{36} \Delta_B$. As mentioned, the choice of this constant enables this family to contain all convex shapes, see proof in SM, Section 6. In fact, for convex targets we have $\Delta \leq 6\Delta_P$ and $\Delta \geq \Delta_B/6$, where Δ is the surface area of the target (SM, Theorem 6.2).

Experiments

In our experiments, we implemented the simulations in the C programming language. The agent was initialized at a random position within \mathbb{T}_n and tasked with searching for a target region $S \subset \mathbb{T}_n$, whose center of mass was fixed at the origin.

Throughout all experiments, we set $d = 1$ and $\ell_{max} = \sqrt[3]{n}/2$. Unlike [Guinard and Korman \(2021\)](#), we did not approximate the step-length distribution using its discrete counterpart. Instead, we employed the Inverse Transform Sampling method to generate floating-point values directly from the continuous probability density function defined in [Eq. \(5\)](#).

Each experiment was repeated at least 200 times. In cases with higher noise, as in [Figs. 4b](#) and [4a](#), the experiments were repeated over 1000 times.

Discrete setting

In the discrete approximation of the Lévy walk we consider a 3D torus graph with n nodes, denoted \mathbb{T}_n , with the searcher moving over it according to a truncated Lévy walk X of parameter μ following the general construction of [Clementi et al. \(2021\)](#). Specifically, in the beginning, the searcher’s initial location is chosen uniformly at random among all nodes in the torus. If the walker is at node u at time t , its next location is determined as follows: first, a length $1 \leq \ell \leq \ell_{max}$ is sampled from the power-law distribution $p(\ell) \propto \ell^{-\mu}$. Next, a node v is chosen uniformly at random from the set of nodes at Manhattan distance ℓ from u . When the transition happens, the actual path followed by the agent to reach the designated node is any shortest path between the source and the destination¹. Hence, the time spent in this step is ℓ . If the agent stays still (because of laziness), the time spent on this step is 0.

Generally, as in the continuous (non-discrete) setting, the reader should keep in mind the distinction between the number of steps complexity (which includes steps where the agent stays still) and the time complexity, which takes into account the duration of each step. In particular, for a given target S , we denote by the *hitting step* $m_{hit}^X(S)$, the number of steps until the searcher detects S , and by $m_{mix}^X(\varepsilon)$ the *mixing step* as the minimum number of steps needed for the total variation distance to the stationary distribution to drop below ε . We use this notion instead of the usual mixing and hitting time to emphasize that it counts steps rather than time. In particular, we write $m_{mix}^X := m_{mix}^X(1/4)$ and note that m_{hit}^X plays the analogous role to m_{detect}^X in the continuous space.

Asymptotic notation

We employ standard Bachmann–Landau notation to capture asymptotic behavior as the torus size $n \rightarrow \infty$. For non-negative functions $f, g : \mathbb{N} \rightarrow [0, \infty)$, we write $f(n) = O(g(n))$ if there exist $c > 0$ and $n_0 \in \mathbb{N}$ such that $f(n) \leq cg(n)$ for all $n \geq n_0$. For example, $n^2 = O(n^3)$ since $n^2 \leq n^3$ for $n \geq 1$. Likewise, $f(n) = \Omega(g(n))$ if $cg(n) \leq f(n)$ for all $n \geq n_0$, for some $c > 0$, $n_0 \in \mathbb{N}$; e.g., $n^3 = \Omega(n^2)$. The notation $f(n) = \Theta(g(n))$ indicates both bounds hold simultaneously, as in $3n^2 + 2n = \Theta(n^2)$.

¹In [Clementi et al. \(2021\)](#), the authors considered a continuous detection setting and therefore defined a probability distribution over the set of shortest paths. However, since we work in the intermittent detection setting, introducing such a distribution is unnecessary.

Data availability

All data used in this study are synthetic and were generated using the simulation and analysis code, which is available at <https://github.com/pragmaticscientist/3D-levy-walks>. Readers can reproduce the datasets using this code.

Code availability

Simulation and analysis code is available at <https://github.com/pragmaticscientist/3D-levy-walks>.

Acknowledgments

The authors thank Dr. Yuwen Wang for helpful discussions. Portions of the manuscript text were edited with the assistance of AI language models (ChatGPT and Gemini) to improve clarity and grammar. Generative AI tools (Perplexity) were also used to assist with code writing, refactoring, and debugging for analysis pipelines. The authors verified all AI-assisted outputs and remain fully responsible for the integrity and accuracy of the work. This work was supported by the Israel Science Foundation (<https://www.isf.org.il>) Grant 1574/24.

Author contributions

Conceptualisation: MS, EN, AK; Methodology: AK; Formal analysis: MS, EN, AK; Simulations: MS; Visualisation: MS; Writing—main document: AK, Writing—SM: MS.

Competing interests

The authors declare no competing interests.

Supplementary Material

1 Model

1.1 Lévy walk process on the Torus

The proof of the following fact is given in the Supplementary Material of [Guinard and Korman \(2021\)](#) (see Claim 2 therein).

Fact 1.1. *Let $\mu \in (1, 3]$ and consider the Lévy walk Z^μ (or X^μ) with maximal step length ℓ_{\max} . The expected step length (and consequently, the expected duration of a single step) $\tau = E(\|V\|)$ scales as*

$$\tau = \begin{cases} \Theta(\ell_{\max}^{2-\mu}), & \text{if } \mu \in (1, 2), \\ \Theta(\log \ell_{\max}), & \text{if } \mu = 2, \\ \Theta(1), & \text{if } \mu \in (2, 3], \end{cases} \quad (6)$$

while the variance σ^2 and the second moment M of the step length satisfy

$$\sigma^2 = \Theta(M) = \begin{cases} \Theta(\ell_{\max}^{3-\mu}), & \text{if } \mu \in (1, 3), \\ \Theta(\log \ell_{\max}), & \text{if } \mu = 3. \end{cases} \quad (7)$$

Recall that in the case of the 3D torus, the maximal step length satisfies $\ell_{\max} = \sqrt[3]{n}/2$.

1.2 Temporal scaling and step-time normalization

We assume that the speed of the process is 1, so that traveling a distance ℓ between two points takes time ℓ time. We further assume that the duration of the scanning phase between successive ballistic displacements takes constant time. In fact, without loss of generality, we may assume that it takes zero time, i.e., $\tau_{\text{scan}} = 0$. Indeed, by Fact 1.1, the expected time required to traverse a single ballistic segment is $\tau = \Omega(1)$, whereas $\tau_{\text{scan}} = \mathcal{O}(1)$. Consequently, the expected time to complete a full step (ballistic displacement plus scanning) satisfies

$$\tau + \tau_{\text{scan}} = \Theta(\tau).$$

Let $T(m)$ denote the total time elapsed after m steps of the walk:

$$T(m) = \sum_{s=1}^m \|V(s)\|,$$

where $V(s) = (V_1(s), V_2(s), V_3(s))$ is the relocation vector chosen at step s , and

$$\|V(s)\| = \sqrt{V_1(s)^2 + V_2(s)^2 + V_3(s)^2}$$

denotes its ℓ_2 -length. Let $m_{\text{detect}}^X(S)$ be the (random) number of steps taken by X until the target S is first detected (equivalently, the first time m such that $X(m) \in S$). By definition, the expected detection time is

$$t_{\text{detect}}^X(S) = \mathbb{E}[T(m_{\text{detect}}^X(S))].$$

2 Preliminary results

In this section, we state several other results that were established in [Guinard and Korman \(2021\)](#) for the two-dimensional scenario, and can be directly extended to the three-dimensional case with minor adaptations to the proofs.

2.1 Time versus number of steps

In the two-dimensional scenario, it was established in [Guinard and Korman \(2021\)](#) that this quantity equals to the expected number of steps until detection $m_{\text{detect}}^X(S)$ multiplied by the mean step duration τ . The same proof also holds in the three-dimensional case, requiring only the substitution of two-dimensional relocation vectors with three-dimensional ones. By the same argument, the result generalizes to arbitrary spatial dimensions. Therefore, the proof is omitted here for brevity.

Formally, the 3D analogue of Claim 3 in the Supplementary Materials in [Guinard and Korman \(2021\)](#) is

Claim 2.1. *For any intermittent random walk X on \mathbb{T}_n and any subset $S \subseteq \mathbb{T}_n$,*

$$t_{\text{detect}}^X(S) = \mathbb{E}[m_{\text{detect}}^X(S)] \cdot \tau,$$

where $\tau = \mathbb{E}[\|V(1)\|]$ denotes the expected step length.

2.2 Monotonicity

A function f on \mathbb{R}^3 is said to be *radial* if there exists a function $\tilde{f} : \mathbb{R}^+ \rightarrow \mathbb{R}$ such that $f(x) = \tilde{f}(\|x\|)$ for every $x \in \mathbb{R}^3$. In this case, f is called *non-increasing* if \tilde{f} is non-increasing. The proof of the following claim follows exactly the same steps as Claim 4 in the Supplementary Materials of [Guinard and Korman \(2021\)](#) and is therefore omitted here.

Claim 2.2. *Let X and Y be independent random variables taking values in \mathbb{R}^3 , with probability density functions f and g , respectively. Let h denote the probability density function of $X + Y$. If both f and g are radial and non-increasing, then h is also radial and non-increasing.*

Corollary 2.3 (Monotonicity). *Let Z be a random walk process on \mathbb{R}^3 , starting at $Z(0) = 0$, with a step-length distribution p . If p is non-increasing, then for any $m \geq 1$ the distribution $p^{Z(m)}$ of $Z(m)$ is radial and non-increasing. In particular, for any*

x, x' points in \mathbb{R}^3 with $\|x'\| \leq \|x\|$, we have $p^{Z(m)}(x) \leq p^{Z(m)}(x')$. Furthermore, for any $x \in \mathbb{R}^3$ and any $m \geq 1$, $p^{Z(m)}(x) \leq \frac{3}{4\pi\|x\|^3}$.

Proof The fact that $p^{Z(m)}$ is radial and non-increasing follows from Claim 2.2 by induction on m . Indeed, the step-length vectors $V(1), V(2), \dots$ are independent and, by hypothesis, admit a radial, non-increasing p.d.f. Hence so does $Z(m) = V(1) + V(2) + \dots + V(m)$. Next, consider $x \in \mathbb{R}^3$ and the ball B of radius $\|x\|$ centered at 0. Note that for every point $y \in B$, we have $\|y\| \leq \|x\|$, and hence, by the fact that $Z(m)$ is radial and non-increasing, we have $p^{Z(m)}(x) \leq p^{Z(m)}(y)$. The upper bound on $p^{Z(m)}(x)$ follows from:

$$1 \geq \int_B p_m^Z(y) dy \geq p_m^Z(x) |B| = p_m^Z(x) \cdot \frac{4\pi}{3} \|x\|^3,$$

completing the proof. \square

2.3 Coordinate projection preserves the Lévy exponent

In this section, we show that the projection of a Lévy walk onto any single axis is itself a Lévy walk, with the same exponent. While a related proof was presented in [Guinard and Korman \(2021\)](#) for the two-dimensional case, our approach generalizes the result to three dimensions and is more naturally extendable to arbitrary dimensions with only minor modifications. In what follows, we denote by Z_1^μ the projection of the Lévy walk Z^μ onto an arbitrary coordinate axis.

Theorem 2.4. *The projection Z_1^μ of Z^μ is a Lévy walk on \mathbb{R} with parameter μ , in the sense that the p.d.f. of the step-lengths of X_1^μ is $p(\ell) \sim 1/\ell^\mu$, for $\ell \in [1, \frac{\ell_{max}}{2}]$. Furthermore, the variance of X_1^μ is*

$$\sigma'^2 = \begin{cases} \Theta(\ell_{max}^{3-\mu}) & \text{if } \mu \in (1, 3) \\ \Theta(\log \ell_{max}) & \text{if } \mu = 3 \end{cases}.$$

Proof It is clear that Z_1^μ is also a random walk that moves incrementally, with the increments between $Z_1^\mu(m)$ and $Z_1^\mu(m+1)$ being the projection $Z_1(m+1)$ of the chosen 3-dimensional vector $V(m+1) = Z^\mu(m+1) - Z^\mu(m)$. These projections are i.i.d. variables as the vectors $(V(m))_m$ are i.i.d. variables, and their signs are \pm with equal probability. Next, we verify that $l_1 := |V_1(1)|$ has a Lévy distribution with parameter μ .

Let V be one step-length drawn according to a Lévy distribution p^μ in the 3-dimensional torus. Recall that the step-length is distributed as:

$$p^\mu(\ell) = \begin{cases} a_\mu & \text{if } \ell \leq 1 \\ a_\mu \ell^{-\mu} & \text{if } \ell \in [1, \ell_{max}) \\ 0 & \text{if } \ell \geq \ell_{max} \end{cases},$$

where a_μ is the normalization factor, with $a_\mu = \frac{1}{1 + \int_1^{\ell_{max}} \ell^{-\mu} d\ell} = \frac{1}{1 + \frac{1 - \ell_{max}^{1-\mu}}{\mu-1}}$. Hence the

distribution of $V = (V_1, V_2, V_3) \in \mathbb{R}^3$ is

$$p^V(v) = \frac{1}{4\pi} \frac{1}{\|v\|^2} p^\mu(\|v\|) = \begin{cases} \frac{a_\mu}{4\pi} \|v\|^{-2} & \text{if } \|v\| \leq 1 \\ \frac{a_\mu}{4\pi} \|v\|^{-\mu-2} & \text{if } \|v\| \in [1, \ell_{max}) \\ 0 & \text{if } \|v\| \geq \ell_{max} \end{cases}. \quad (8)$$

Recall that $l_1 := |V_1(1)|$ is the distribution of the length of a projected step onto the first coordinate. Let $v = (v_1, v_2, v_3)$ denote a realization of the random vector V . For $v_1 \in (0, \ell_{max})$, we have

$$p^{l_1}(v_1) = 2 \int_I p^V(v) dv = \frac{a_\mu}{2\pi} \int_I \left[\mathbf{1}(\|v\| < 1) \frac{1}{\|v\|^2} + \mathbf{1}(\|v\| \geq 1) \frac{1}{\|v\|^{\mu+2}} \right] dv,$$

where $I \subset \mathbb{R}^3$ comprises all vectors v whose total length is constrained by a maximum step size ℓ_{max} and the first entry is equal to v_1 (i.e. I is disc in the plane orthogonal to v_1 , centered at v_1 , and of radius $\sqrt{\ell_{max}^2 - v_1^2}$). Formally, we define this set as:

$$I = \left\{ v \in \mathbb{R}^3 : P_x(v) = v_1 \text{ and } \|P_{y,z}(v)\| \leq \sqrt{\ell_{max}^2 - v_1^2} \right\}.$$

Here, P_x denotes the projection onto the x -axis, while $P_{y,z}$ represents the projection onto the yz -plane. The inequality governing the yz -component is derived directly from the Euclidean norm; because the total magnitude $\|v\|$ cannot exceed ℓ_{max} , the magnitude of the lateral projection is geometrically restricted by the remaining length available after accounting for the longitudinal component v_1 . Now assume $|v_1| \geq 1$ and observe that this implies $\|v\| \geq 1$. Hence,

$$p^{l_1}(v_1) = \frac{a_\mu}{2\pi} \int_I \frac{1}{\|v\|^{\mu+2}} dv = \frac{a_\mu}{2\pi} \int_I \frac{1}{v_1^{\mu+2} \left[1 + \left(\frac{v_2}{v_1}\right)^2 + \left(\frac{v_3}{v_1}\right)^2 \right]^{\frac{\mu+2}{2}}} dv. \quad (9)$$

Note that Equation (9) is a surface integral. Thus, we can evaluate it by parameterizing the surface using the mapping $\mathbf{r}(w_1, w_2) = (v_1, v_1 w_1, v_1 w_2)$ and applying the standard formula for a surface integral over a parameterized region D :

$$\int_I f(v) dA(x) = \int_D f(\mathbf{r}(w_1, w_2)) \left\| \frac{\partial \mathbf{r}}{\partial w_1} \times \frac{\partial \mathbf{r}}{\partial w_2} \right\| dw_1 dw_2.$$

where $dA(x)$ denotes an infinitesimal surface element at the point x on the surface I and $D = \mathbf{r}^{-1}(I)$ is the domain of the parameters w_1 and w_2 . By substituting our specific parameterization into this expression, we can transform the integral into the w -coordinate system to simplify the subsequent calculations. Thus, $\frac{\partial \mathbf{r}}{\partial w_1} = v_1(0, 1, 0)^\top$, $\frac{\partial \mathbf{r}}{\partial w_2} = v_1(0, 0, 1)^\top$ and $\left\| \frac{\partial \mathbf{r}}{\partial w_1} \times \frac{\partial \mathbf{r}}{\partial w_2} \right\| = \|(v_1^2, 0, 0)^\top\| = v_1^2$. To conclude this step, we observe that the change of variables $v_2 = v_1 w_1$ and $v_3 = v_1 w_2$ allows us to represent the set I as the image of a simplified domain D under the mapping \mathbf{r} . Specifically, $I = \mathbf{r}(D)$, where D is defined as the disk:

$$D = \left\{ w \in \mathbb{R}^2 : \|w\| \leq \sqrt{\frac{\ell_{max}^2}{v_1^2} - 1} \right\}.$$

In fact, for any $w \in D$, the parameterization $\mathbf{r}(w) = (v_1, v_1 w_1, v_1 w_2)$ satisfies the required conditions for D . First, the longitudinal component is fixed at v_1 . Second, the total magnitude satisfies the bound $\|\mathbf{r}(w)\|^2 = v_1^2(1 + w_1^2 + w_2^2) = v_1^2(1 + \|w\|^2) \leq \ell_{max}^2$, ensuring that the vector remains within the maximum step length. Therefore, we can rewrite the previous integral as follows:

$$p^{l_1}(v_1) = \frac{a_\mu}{2\pi} \int_D \frac{v_1^2}{v_1^{\mu+2} (1 + \|y\|^2)^{\frac{\mu+2}{2}}} dy = \frac{a_\mu}{2\pi v_1^\mu} \int_D \frac{1}{(1 + \|y\|^2)^{\frac{\mu+2}{2}}} dy.$$

Now we focus on the remaining integral and show that it is upper bounded by a constant. Indeed,

$$\int_D \frac{1}{(1 + \|y\|^2)^{\frac{\mu+2}{2}}} dy \leq \int_{\mathbb{R}^2} \frac{1}{(1 + \|y\|^2)^{\frac{\mu+2}{2}}} dy = \mathcal{O}(1).$$

In fact, since $\mu > 1$, we have that $\frac{\mu+2}{2} \geq 1$. To see why the integral evaluates to a constant, we change to polar coordinates. Let $y = (r \cos \theta, r \sin \theta)$, so that $\|y\| = r$ and the area element is $dy = r dr d\theta$. The integral over \mathbb{R}^2 becomes:

$$\begin{aligned} \int_{\mathbb{R}^2} \frac{1}{(1 + \|y\|^2)^{\frac{\mu+2}{2}}} dy &= \int_0^{2\pi} \int_0^\infty \frac{r}{(1 + r^2)^{\frac{\mu+2}{2}}} dr d\theta \\ &= 2\pi \int_0^\infty r(1 + r^2)^{-\frac{\mu+2}{2}} dr. \end{aligned}$$

By applying the substitution $u = 1 + r^2$ (with $du = 2r dr$), the integral simplifies to:

$$\begin{aligned} \pi \int_1^\infty u^{-\frac{\mu+2}{2}} du &= \pi \left[\frac{u^{1-\frac{\mu+2}{2}}}{1-\frac{\mu+2}{2}} \right]_1^\infty \\ &= \pi \left[\frac{u^{-\mu/2}}{-\mu/2} \right]_1^\infty. \end{aligned}$$

Since $\mu > 1$, the term $u^{-\mu/2}$ vanishes as $u \rightarrow \infty$. Evaluating at the limits gives:

$$\pi \left(0 - \frac{1}{-\mu/2} \right) = \frac{2\pi}{\mu}.$$

Because μ is a fixed parameter, the result $\frac{2\pi}{\mu}$ is independent of v_1 , and therefore the expression is indeed $\mathcal{O}(1)$. Hence, for $|v_1| \geq 1$, Equation (9) can be rewritten as

$$p^{l_1}(v_1) = \mathcal{O}(1/v_1^\mu).$$

The final stage of the proof establishes that $p^{l_1}(v_1) = \Omega(1/v_1^\mu)$ holds within the restricted domain $|v_1| \leq \frac{\ell_{\max}}{2}$. Under this assumption – specifically that v_1 lies in this central sub-interval – we observe that

$$p^{l_1}(v_1) = \frac{a_\mu}{2\pi v_1^\mu} \int_D \frac{1}{(1 + \|y\|^2)^{\frac{\mu+2}{2}}} dy \geq \frac{a_\mu}{2\pi v_1^\mu} \int_{D'} \frac{1}{(1 + \|y\|^2)^{\frac{\mu+2}{2}}} dy$$

where $D' = \{y \in \mathbb{R}^2 : \|y\| \leq 1\}$ and the inequality follows from $D' \subseteq D$ for $|v_1| \leq \frac{\ell_{\max}}{2}$.

To conclude, observe that $\int_{D'} \frac{1}{(1 + \|y\|^2)^{\frac{\mu+2}{2}}} dy$ is a positive constant. Thus, we have that

$p^{l_1}(v_1) = \Theta(1/v_1^\mu)$ for $v_1 \in [1, \ell_{\max}/2]$ and $p^{l_1}(v_1) = \mathcal{O}(1/v_1^\mu)$ for $v_1 \in [\ell_{\max}/2, \ell_{\max}]$. To prove the claim about the variance of the projected random walk, we followed exactly the same steps as in [Guinard and Korman \(2021\)](#) (Supplementary Material, Theorem 6); hence, we omit the rest of the proof. \square

3 Universal Lower Bound

In this section, we establish [Theorem 3.1](#), which states that the expected detection time of any compact target S is $\Omega(n/\Delta_B)$. Here, $\Delta_B = \Delta_B(S)$ denotes the *largest face area* of S , namely, the surface area of largest face of the box $B = \text{Box}(S)$ that minimizes surface area while containing S (red shape in [Fig. 2c](#)). This lower bound is universal to any search strategy; consequently, it applies to any Lévy walk regardless of the exponent μ , even under continuous detection.

Theorem 3.1. *Let X be any search process on the torus. Consider any compact target S , then the expected time to detect S is $\Omega(n/\Delta_B)$ where Δ_B denotes the largest face area of the bounding box of S .*

Proof For simplicity, assume B is axis-aligned with side lengths $x_1 \leq x_2 \leq x_3$ along the main axes, where $x_1 \geq 2$ because the detection radius satisfies $d \geq 1$ (see Methods Section 2). Consider an enlarged box B' with side lengths $3x_1, 3x_2, 3x_3$ and tile the torus with copies of B' (See Figure 2c for a visual representation), placing adjacent boxes exactly x_1 apart along each axis. This yields M boxes, with

$$M = \Theta\left(\frac{n}{x_1 x_2 x_3}\right).$$

Recall that our model has a fixed target S and initial searcher position $X(0)$ uniform on \mathbb{T}_n . This is equivalent (by translation invariance) to having a fixed initial position at the origin, i.e., $X(0) = 0$, and a uniform center of mass x^* . Thus, the probability that the target is fully contained in the i -th box B'_i is $\mathbb{P}(S \subseteq B'_i) = x_1 x_2 x_3 / n = \Theta(1/M)$, indeed the subset of B' where x^* could lie is a box with sides x_1, x_2 and x_3 (it is a copy of B placed in the center of B'). So, the probability that the target belongs to some box is a constant:

$$\mathbb{P}(S \subseteq \bigcup_i^M B'_i) = \sum_i^M x_1 x_2 x_3 / n = \Theta(1).$$

Hence, by law of total expectation, it suffices to lower bound the expected time to find S , conditioning on S being fully contained within some box B' .

Moreover, conditioning on this event, each box has equal probability to contain the target, since all boxes are identical, up to translation in space. The target box B^* containing the target is therefore uniformly distributed over $\{B'_1, \dots, B'_M\}$.

Fix a search strategy X , and consider a single realization of it, which induces an ordering of the boxes according to the times at which they are first visited; we denote this sequence by $\text{Seq}(X) = (b_1, \dots, b_M)$; note that different realizations of a randomized strategy may produce different sequences. Since the target box is chosen uniformly at random, its expected position in any such sequence is $(M+1)/2$. Averaging over all choices of B^* and all realizations of X , it follows that, in expectation, X must visit $\Omega(M)$ distinct boxes before entering B^* . Moreover, traveling between two distinct boxes requires time $\Omega(x_1)$. It follows that

$$\mathbb{E}[t_{\text{detect}}^X(S) \mid S \subseteq \bigcup_i^M B'_i] = \Omega(x_1 M) = \Omega\left(\frac{n}{x_2 x_3}\right).$$

Recalling that $\Delta_B = x_2 x_3$ completes the proof. \square

4 Lower Bounds for Non-Cauchy Lévy Walks

In this section, we derive lower bounds on the detection time of Lévy walks that do not follow the Cauchy distribution. Specifically, for $1 < \mu < 2$, we show that the corresponding intermittent Lévy walks are inefficient at locating targets of small surface area. Conversely, for $2 < \mu \leq 3$, we demonstrate that these Lévy walks perform poorly when detecting targets of large surface area, except when they are line-shaped.

To this end, we introduce the quantity T_d , the first time the process is expected to leave the ball of radius d . In the intermittent setting, it denotes the time in which the endpoint of a step exits the ball of radius d centered at the starting point. Note that T_d provides a lower bound on the time required to detect a target located at distance d or greater.

Recall that $B = \text{Box}(S)$ denotes the bounding box of S of minimum surface area, with side lengths $x_1 \leq x_2 \leq x_3$, where we assume without loss of generality that B is aligned with the coordinate axes (See Figure 2c for a visual representation).

Theorem 4.1. *Let X be any search process on the torus. Consider any compact target S with a bounding box $B = \text{Box}(S)$ of largest surface area Δ_B and $\delta \in [\frac{1}{2}, 1]$ such that $x_3 = \Delta_B^\delta$ and $x_2 = \Delta_B^{1-\delta}$, then the expected time to detect S is*

$$\Omega \left(\frac{n}{\Delta_B^{2-\delta}} T_{\Delta_B^{1-\delta}} \right).$$

Proof Consider an enlarged box B' with side lengths $3x_1$, $3x_2$, and $3x_3$. Tile the torus with copies of B' as in the proof of Theorem 3.1, positioning them so that any two adjacent boxes are separated by a distance of exactly $x_2 = \Delta_B^{1-\delta}$. This yields

$$\Theta \left(\frac{n}{(x_1 + \Delta_B^{1-\delta})(x_2 + \Delta_B^{1-\delta})(x_3 + \Delta_B^{1-\delta})} \right) = \Theta \left(\frac{n}{\Delta_B^{1-\delta} x_2 x_3} \right) = \Theta \left(\frac{n}{\Delta_B^{2-\delta}} \right)$$

such boxes. Next, by the same reasoning used in the proof of Theorem 3.1, even if the searcher is aware of this tiling, it must examine at least half of these boxes on average before finding the one that contains the target. Moving from one box to the next requires time $T_{\Delta_B^{1-\delta}}$, so the expected detection time is

$$\Omega \left(\frac{n}{\Delta_B^{2-\delta}} T_{\Delta_B^{1-\delta}} \right),$$

concluding the theorem. \square

4.1 Lower bounds for Lévy walks with $1 < \mu < 2$

Recall that $m_{\text{detect}}^{X^\mu}(S)$ denotes the number of steps needed by the Lévy walk with exponent μ to hit the target. The following claim provides a lower bound for the number of steps, which holds for any exponent $\mu \in (1, 3]$. The proof is deferred to Section 4.1.1.

Claim 4.2. *Consider an intermittent Lévy walk X^μ with $\mu \in (1, 3]$ and a target S . Then,*

$$\mathbb{E}[m_{\text{detect}}^{X^\mu}(S)] = \Omega \left(\frac{n}{V} \right),$$

where V denotes the volume of S .

Due to a variant of Wald's identity (see Claim 2.1), multiplying this lower bound by the average step length of a given Lévy walk yields a lower bound on the detection time for this Lévy process. As given by Eq. (6), for $\mu \in (1, 2)$, the average step length is $\Theta(n^{\varepsilon/3})$, implying the following lower bound on the detection time:

Theorem 4.3. *Consider a target S of volume V . The detection time of an intermittent Lévy walk with $\mu \in (1, 2)$ is:*

$$t_{\text{detect}}^{X^\mu}(S) = \Omega \left(\frac{n^{1+\varepsilon/3}}{V} \right).$$

4.1.1 Proof of Claim 4.2

Proof Recall that the searcher starts from a random point of the torus, which is equivalent to initially let it start at the origin, and locate the target's center of mass uniformly at random in the torus. Denote the target with its center of mass at the point x by $S(x)$. Similarly, define $R_t := X(t) - S(0)$, the reflection of the target centered at $X(t)$. Observe that if, at time t , the Lévy walk is at a location $X(t) \notin S$, then R_t coincides with the set of positions at which the center of mass of the target cannot be located. Indeed, we have

$$\begin{aligned} X(t) \in S(x) &\iff \exists w \in S(x) \text{ such that } w = X(t) \\ &\iff \exists w \in S(0) \text{ such that } x + w = X(t) \\ &\iff \exists w \in S(0) \text{ such that } x = X(t) - w \\ &\iff x \in R_t. \end{aligned}$$

Now, define the set

$$F_t := \bigcup_{j=0}^t R_j, \quad (10)$$

which is obtained by taking the union of all regions excluded at each time step $j \leq t$, and therefore contains every point that cannot be the target's center of mass after t steps without hitting the target. Observe that, for each j ,

$$\text{Vol}(R_j) \leq V.$$

Indeed, R_t results from a reflection and a shift of S , and hence has the same volume. Thus, we can compute the following upper bound to the volume of F_t :

$$\text{Vol}(F_t) = \text{Vol}\left(\bigcup_{j=0}^t R_j\right) \leq \sum_{j=0}^t \text{Vol}(R_j) \leq (t+1)V.$$

Next, we show that when $t < \frac{n}{2V}$,

$$\mathbb{P}(m_{\text{detect}}^{X^\mu}(S) = t \mid m_{\text{detect}}^{X^\mu}(S) \geq t) = \mathcal{O}\left(\frac{V}{n}\right).$$

Recall that $m_{\text{detect}}^{X^\mu}(S)$ denotes the number of steps for the Lévy walk X^μ before it hits the target S , then $m_{\text{detect}}^{X^\mu}(S) \geq t$ indicates that the target was not found in the first $t-1$ steps. Moreover, since the center of mass of the target is chosen uniformly at the start of the search, it follows that after $t-1$ unsuccessful steps the conditional distribution of S at step t is uniform over $\mathbb{T} \setminus F_{t-1}$, which has volume at least

$$n - tV \geq n - \frac{n}{2} = \frac{n}{2}.$$

Moreover, Eq. (10) guarantees that the set of possible locations for the target center has volume at most V . Therefore, the probability can be bounded as

$$\mathbb{P}(m_{\text{detect}}^{X^\mu}(S) = t \mid m_{\text{detect}}^{X^\mu}(S) \geq t) \leq \frac{2V}{n}.$$

This shows that, for $t < n/(2V)$, the probability of hitting the target in a single step is at most twice the fraction of the state space occupied by the target. We now lower bound the expectation of $m_{\text{detect}}^{X^\mu}(S)$. By definition,

$$\mathbb{E}[m_{\text{detect}}^{X^\mu}(S)] = \sum_{t=1}^{\infty} \mathbb{P}(m_{\text{detect}}^{X^\mu}(S) \geq t).$$

Observe that the probability that the target has not been found by time t can be bounded below as

$$\mathbb{P}(m_{\text{detect}}^{X^\mu}(S) \geq t) = \prod_{j=0}^{t-1} \left(1 - \mathbb{P}(m_{\text{detect}}^{X^\mu}(S) = j+1 \mid m_{\text{detect}}^{X^\mu}(S) > j)\right) \geq \left(1 - \frac{2V}{n}\right)^t.$$

This tail lower bound means the distribution has at least geometric decay, implying

$$\mathbb{E}[m_{\text{detect}}^{X^\mu}(S)] \geq \sum_{t=1}^{\infty} (1 - 2V/n)^t \geq \frac{1 - 2V/n}{2V/n} = \frac{n}{2V} - 1,$$

which completes the proof. \square

4.2 Lower bounds for Lévy walks with $2 < \mu \leq 3$

The following claim concerns a general random walk process on the 3D torus and thus applies not only to our main subject of interest—the Lévy walk—but also to other search processes.

Claim 4.4. *Consider a random walk process X on the torus \mathbb{T}_n and let σ' denote the standard deviation of the length of the projected steps onto one of the coordinates.*

- *For every step $m \in \mathbb{N}$, $\max_{s \leq m} \|X(s) - X(0)\| = O(\sqrt{m}\sigma')$.*
- *Let m_d be the number of steps needed to go to distance at least $d < \sqrt[3]{n}/2$, in other words, m_d is the first step m for which $\|X(m) - X(0)\| \geq d$. We have $\mathbb{E}(m_d) = \Omega(d^2/\sigma'^2)$.*
- *If the process is intermittent and τ denotes the average length of a jump, then the expected time before reaching distance $d < \sqrt[3]{n}/2$ is $T_d = \Omega(d^2/\sigma'^2\tau)$.*

In particular, if the process is intermittent and L is the maximal length in the support of the step-length distribution, then the expected time needed to go to a distance $\Omega(\sqrt{n})$ is $\Omega(\frac{n}{L})$.

Proof The proof of the claim is similar to the corresponding proof in [Guinard and Korman \(2021\)](#) (Claim 10 in the Supplementary Materials), except for minor adaptations to the 3D setting. We nevertheless include the proof here.

Given the search process X on the torus, let Z be the process on \mathbb{R}^3 , with $Z(0) = X(0)$ and evolving with the same relocation vectors as X (except that Z does not wrap around the torus due to the boundary conditions). Since the distance between $Z(m)$ and $Z(0)$, in \mathbb{R}^3 , is always at least that of $X(m)$ and $X(0)$, in \mathbb{T}_n , the number of steps needed to go to distance d in \mathbb{T}_n is at least as high as in \mathbb{R}^3 . Hence, we may analyze the process Z instead of X .

Define $d_{\text{max}}^Z(m)$ as the maximal distance (from the initial point) that the process Z reached from step 0 up to step m , i.e.,

$$d_{\text{max}}^Z(m) = \max_{s \leq m} \|Z(0) - Z(s)\|.$$

Now write $Z = (Z_1, Z_2, Z_3)$, let p' be the p.d.f. of the projected step-lengths (i.e., the p.d.f. of the step-lengths of Z_i , for any $i \in \{1, 2, 3\}$), and let τ' and σ' be respectively its mean and standard deviation. Next, let $d_{i,\text{max}}^Z(m)$ be the maximal distance reached by the projection

on coordinate $i = 1, 2, 3$. Since steps are independent, the standard deviation of $Z_i(s)$, for $s \leq m$, is $\sqrt{s}\sigma' \leq \sqrt{m}\sigma'$. By Kolmogorov's inequality, we have for any $\lambda > 0$,

$$\Pr(d_{i,max}^Z(m) \geq \lambda\sqrt{m}\sigma') \leq \frac{1}{\lambda^2}.$$

Furthermore, since $d_{max}^Z(m) \leq \sqrt{3} \max\{d_{1,max}^Z(m), d_{2,max}^Z(m), d_{3,max}^Z(m)\}$, we have by a union bound argument, that for any $\lambda > 0$,

$$\Pr(d_{max}^Z(m) \geq \lambda\sqrt{m}\sigma') \leq \sum_{i=1,2,3} \Pr\left(d_{i,max}^Z(m) \geq \frac{\lambda}{\sqrt{3}}\sqrt{m}\sigma'\right) \leq \frac{9}{\lambda^2}.$$

Hence,

$$\begin{aligned} \mathbb{E}(d_{max}^Z(m)) &= \int_{s=0}^{\infty} \Pr\left(d_{max}^Z(m) \geq s\right) ds = \sum_{\lambda=0}^{\infty} \int_{\lambda'=0}^{\sqrt{m}\sigma'} \Pr\left(d_{max}^Z(m) \geq \lambda\sqrt{m}\sigma' + \lambda'\right) d\lambda' \\ &\leq \sqrt{m}\sigma' \left(\sum_{\lambda \geq 0} \Pr(d_{max}^Z(m) \geq \lambda\sqrt{m}\sigma') \right) = O(\sqrt{m}\sigma'), \end{aligned} \quad (11)$$

where the second equality is due to separating the integration into the intervals of width $\sqrt{m}\sigma'$ and the inequality is due to setting $\lambda' = 0$ for each interval. Eq. (11) proves the first item of Claim 4.4.

Next, write the m_d of the statement as m_d^X , to distinguish it from the similarly defined m_d^Z , which is the first step for which $\|Z(m) - Z(0)\| \geq d$. As remarked above, we have $m_d^X \geq m_d^Z$. Note that for $m \geq m_d^Z$, we have $d_{max}^Z(m) \geq d_{max}^Z(m_d) \geq d$. Therefore, by Markov's inequality,

$$\mathbb{E}\left(d_{max}^Z(2\mathbb{E}(m_d^Z))\right) \geq \mathbb{E}\left(d_{max}^Z(2\mathbb{E}(m_d^Z)) \mid m_d^Z < 2\mathbb{E}(m_d^Z)\right) \cdot \Pr\left(m_d^Z < 2\mathbb{E}(m_d^Z)\right) \geq d \cdot \frac{1}{2}. \quad (12)$$

Now using Eq. 11 with $m = 2\mathbb{E}(m_d^Z)$, we have $\mathbb{E}(d_{max}^Z(2\mathbb{E}(m_d^Z))) = O(\sqrt{\mathbb{E}(m_d^Z)}\sigma')$ and hence, by Eq. 12,

$$\mathbb{E}(m_d^X) \geq \mathbb{E}(m_d^Z) = \Omega\left(\frac{d^2}{\sigma'^2}\right),$$

which proves the second item of Claim 4.4.

The last item in the claim is a lower bound on $T_d = \mathbb{E}(T(m_d^X))$, the expected time that X needs to reach distance d , assuming that X is intermittent. To obtain it, we observe that m_d^X is the hitting step of the set of nodes at distance d or more in the torus. Hence, by Claim 2.1, we have $T_d = \mathbb{E}(m_d^X) \cdot \tau \geq \mathbb{E}(m_d^Z) \cdot \tau = \Omega\left(\frac{d^2}{\sigma'^2}\tau\right)$, which is exactly as needed.

Finally, observe that

$$\sigma'^2 = \int_0^L p'(\ell)\ell^2 d\ell \leq L \int_0^L p'(\ell)\ell d\ell = L\tau' \leq L\tau, \quad (13)$$

where the last inequality is justified by the fact that the projection reduces distances. This completes the proof of Claim 4.4. \square

Towards proving the lower bound for $\mu \in (2, 3]$, we first establish the following.

Claim 4.5. *Let X^μ be an intermittent Lévy walk process on the torus \mathbb{T}_n , for some fixed $\mu \in (2, 3]$. The expected time required to reach a distance of $d \geq 1$ from the starting point is:*

$$T_d = \begin{cases} \Omega(d^{\mu-1}) & \text{if } \mu \in (2, 3) \\ \Omega\left(\frac{d^2}{\log d}\right) & \text{if } \mu = 3 \end{cases}.$$

The proof for the claim in the intermittent setting is identical to that of Claim 13 in the Supplementary Materials of [Guinard and Korman \(2021\)](#), so we omit it. Notably, the argument relies on Theorem 2.4, even though that theorem is stated for \mathbb{R} while the present claim concerns the torus \mathbb{T}_n . This link is made precise by Claim 4.4, which provides a lower bound on the time required to reach distance d in terms of the mean step length and the projected variance of a single step length.

Theorem 4.6. *Let $\mu \in (2, 3]$ and let Δ_B be the largest face area of the bounding box $B = \text{Box}(S)$ containing a compact target S with $\delta \in [\frac{1}{2}, 1]$ such that $x_3 = \Delta_B^\delta$ and $x_2 = \Delta_B^{1-\delta}$. Write $\mu = 2 + \epsilon$. The detection time of the intermittent Lévy walk X^μ with respect to a target S is*

$$t_{\text{detect}}^{X^\mu}(S) = \begin{cases} \Omega\left(n\Delta_B^{\epsilon(1-\delta)-1}\right) & \text{if } \mu \in (2, 3) \\ \Omega\left(\frac{n}{\Delta_B^\delta \log \Delta_B}\right) & \text{if } \mu = 3 \end{cases}.$$

Proof The Theorem follows by combining the lower bound $\Omega\left(\frac{n}{\Delta_B^{2-\delta}} T_{\Delta_B^{1-\delta}}\right)$ given by Theorem 4.1 with the lower bound on T_d given by Claim 4.5. Specifically, for the case where $\mu \in (2, 3)$, we obtain:

$$\Omega\left(\frac{n}{\Delta_B^{2-\delta}} T_{\Delta_B^{1-\delta}}\right) = \Omega\left(\frac{n}{\Delta_B^{2-\delta}} \Delta_B^{(1-\delta)(\epsilon+1)}\right) = \Omega(n\Delta_B^{\epsilon(1-\delta)-1}),$$

which matches the desired result. On the other hand, for $\mu = 3$, the expression becomes:

$$\Omega\left(\frac{n}{\Delta_B^{2-\delta}} T_{\Delta_B^{1-\delta}}\right) = \Omega\left(\frac{n\Delta_B^{2(1-\delta)}}{\Delta_B^{2-\delta}(1-\delta)\log \Delta_B}\right) = \Omega\left(\frac{n}{\Delta_B^\delta \log \Delta_B}\right).$$

This completes the derivation for the second case and concludes the proof. \square

Since the elongation of a disc or a ball is $\delta = 1/2$, the above theorem implies the following.

Corollary 4.7. *Let $\mu \in (2, 3]$ and consider either a ball or a disc target S of surface area Δ . The detection time of the intermittent Lévy walk X^μ with respect to S is*

$$t_{\text{detect}}^{X^\mu}(S) = \begin{cases} \Omega\left(n\Delta^{\epsilon/2-1}\right) & \text{if } \mu \in (2, 3) \\ \Omega\left(\frac{n}{\Delta^{1/2} \log \Delta}\right) & \text{if } \mu = 3 \end{cases}.$$

4.3 The δ of a line target

When the raw target is a line segment of length L , the corresponding target region is a cylindrical shape with radius equal to the detection radius $d \geq 1$. For this class of targets, the area of the bounding box $B = \text{Box}(S)$ satisfies $\Delta_B = x_3 x_2$, where the largest side is $x_3 = L + 2d$ and the second largest side is $x_2 = 2d$. By the definition of δ , it follows that

$$\Delta_B^\delta = x_3 = \frac{\Delta_B}{2d}.$$

Taking the logarithm with base Δ_B on both sides yields

$$\delta = 1 - \frac{\log(2d)}{\log(\Delta_B)}.$$

Since $\Delta_B \geq (2d)^2$, it follows that the parameter δ is always bounded below by $\frac{1}{2}$.

5 The Detection time of the Cauchy Walk

In this section, we aim to prove Theorem 5.4, which states that the expected time required for the Cauchy walk to find a target S is $\mathcal{O}(n \log^3 n / \Delta_P)$. Here, $\Delta_P = \Delta_P(S)$ denotes the *projected surface area* of the target—defined as the maximum of the areas of the projections of S onto each of the six faces of the minimum surface area bounding box $B = \text{Box}(S)$. We begin with the following lemma, whose proof is identical to the proof of Lemma 19 in Guinard and Korman (2021), and is therefore omitted from this manuscript.

Lemma 5.1. *Consider a random walk process Z on \mathbb{R}^3 and its projection X on the torus \mathbb{T}_n and denote by Z^{z_0} the process Z starting at $Z(0) = z_0$. Let $S \subset \mathbb{T}_n$, then for any integer m_0 we have*

$$\mathbf{E}(m_{\text{detect}}^X(S)) = \mathcal{O}\left(m_0 \cdot \frac{\sup_{z_0 \in S} \sum_{m=0}^{m_0} \Pr(Z^{z_0}(m) \in S)}{\sum_{m=m_0}^{2m_0} \Pr(Z(m) \in S)}\right). \quad (14)$$

5.1 Technical lemmas and claims

Next, we present two lemmas, analogous to Lemmas 20 and 21 in Guinard and Korman (2021), whose proofs require only minor modifications. The full proofs are deferred to Section 5.3.

Lemma 5.2. *For any constant $\alpha > 0$, there exist a constant $c > 0$ such that for any integer $m \in [1, \alpha \ell_{\max}]$, and any $x \in \mathbb{R}^3$, with $\|x\| \leq m$,*

$$p^{Z(m)}(x) \geq \frac{c}{m^3}. \quad (15)$$

Lemma 5.3. *For any constant $\alpha > 0$, there exists a constant $c' > 0$ such that, for any integer $m \in [2, \alpha \ell_{\max}]$, and for any $x \in \mathbb{R}^3$, we have*

$$\Pr(Z(m) \in B(x)) \leq \frac{c' \log^3 m}{m^3}. \quad (16)$$

5.2 Optimal hitting time

Now we can use all the claims and lemmas above to prove the following theorem.

Theorem 5.4. *Consider the Cauchy walk X^{cauchy} on the torus. The hitting time of the walk with respect to a compact target S of projected surface area Δ_P is*

$$t_{\text{detect}}^{X^{\text{cauchy}}}(S) = \mathcal{O}\left(\frac{n \log^3 n}{\Delta_P}\right). \quad (17)$$

Proof By definition of *projected surface area*, there exists a projection π onto one face of the bounding box $B = \text{Box}(S)$ such that $\text{Area}(\pi(S)) = \Delta_P$. Moreover, following [Vershynin \(2018\)](#), the 3-packing number of any two-dimensional set with area Δ_P is at least $c\Delta_P$ where c is a universal constant. Here, the 3-packing number refers to the maximum cardinality of a subset of points where each pair is separated by a distance of at least 3. Let $S^{\text{proj}} \subseteq \pi(S)$ be a set of points realizing the packing number. For each $w \in S^{\text{proj}}$, we define its pre-image under the projection, $\pi^{-1}(w)$, as the point in S closest to the projection plane:

$$\pi^{-1}(w) = \arg \min\{d(w, w') : w' \in S, \pi(w') = w\}.$$

For each $w' \in \pi^{-1}(S^{\text{proj}})$, we select a point $x \in S$ such that $\|x - w'\| = 1$ and the distance from x to the surface of S is at least 1. The existence of such a point follows directly from the definition of target, given the assumption $d \geq 1$ for the detection radius. Let $S^* \subset S$ denote the set of these chosen points. Since projections are non-expansive (i.e., they do not increase distances), the mapping from S^{proj} to S^* is injective, and thus $|S^*| = |S^{\text{proj}}| = c\Delta_P$. Observe that the union of balls $B(S^*)$ is contained in S . Consequently, $\mathbb{E}(t_{\text{detect}}^X(S)) \leq \mathbb{E}(t_{\text{detect}}^X(B(S^*)))$, therefore we focus on $B(S^*)$.

Recall from [Claim 2.1](#) that $\mathbb{E}(t_{\text{detect}}^X(B(S^*))) = \mathbb{E}(m_{\text{detect}}^X(B(S^*))) \tau$, where τ is the expected step length of the random process. Thus, we can prove our theorem by giving an upper bound to [Eq. 14](#) ([Lemma 5.1](#)) applied to $B(S^*)$ with $m_0 = \sqrt[3]{n}$. We begin by lower bounding the denominator, then we proceed by upper bounding the numerator.

Lower bound for the denominator in [Eq. 14](#).

Note that any $x \in B(S^*)$ trivially satisfies $\|x\| \leq m$ for any $m \geq m_0 + 1$, because m_0 was chosen to be slightly more than the diameter of the torus. Therefore, we can apply [Lemma 5.2](#) to get a lower bound on the denominator.

$$\begin{aligned} \sum_{m=m_0+1}^{2m_0} \Pr(Z(m) \in B(S^*)) &= \sum_{m=m_0+1}^{2m_0} \int_{x \in B(S^*)} p_m^Z(x) dv \\ &\geq \sum_{m=m_0+1}^{2m_0} \frac{c}{m^3} |B(S^*)| = \Omega\left(\frac{\Delta_P}{n^{2/3}}\right). \end{aligned}$$

Upper bound for the numerator in Eq. 14.

Next, we provide an upper bound to the numerator of the r.h.s of Eq. 14 which is the expected number of returns to $B(S^*)$ within the first m_0 steps, conditioning on the fact that $Z(0) = z$, for some $z \in B(S^*)$. Let us denote this process by Z^z (note that $Z = Z^0$). Then,

$$\sum_{m=0}^{m_0} \Pr(Z^z(m) \in B(S^*)) \leq 2 + \sum_{m=2}^{m_0} \Pr(Z^z(m) \in B(S^*)).$$

Clearly, the probability density function $p^{Z^z(m)}$ of $Z^z(m)$ is obtained by a translation from $p^{Z(m)}$. Thus, by Corollary 2.3, we have for any $y \in \mathbb{R}^3$:

$$p^{Z^z(m)}(y) = \mathcal{O}\left(\frac{1}{\|y - z\|^3}\right).$$

In particular, for y such that $\|y - z\| \geq 2$,

$$\Pr(Z^z(m) \in B(y)) = \mathcal{O}\left(\frac{1}{(\|y - z\| - 1)^3}\right)$$

Next, denote by $x_z \in S^*$ the point whose ball contains z . Now, let $r > 0$ be a value that we define later and let us denote by $S_{\leq r}^*$ the subset of S^* whose points are at distance at most r from x_z . Analogously, define $S_{> r}^* \equiv S^* \setminus S_{\leq r}^*$. We proceed with the following decomposition:

$$\Pr(Z^z(m) \in B(S^*)) = \Pr(Z^z(m) \in B(S_{> r}^*)) + \Pr(Z^z(m) \in B(S_{\leq r}^*)).$$

Note that $|\{w \in \pi(S^*) : \|w - \pi(x_z)\| \leq r\}| \leq 4r^2$, thus by the non-expansiveness of the projections we have $|S_{\leq r}^*| \leq 4r^2$. Hence, using Lemma 5.3 we get:

$$\Pr(Z^z(m) \in B(S_{\leq r}^*)) = \mathcal{O}\left(\frac{r^2 c' \log^3 m}{m^3}\right).$$

Next, we aim to upper bound $\Pr(Z^z(m) \in B(S_{> r}^*))$. By the triangle inequality, for any $x \in S_{> r}^*$, we have $\|x - z\| \geq \|x - x_z\| - 1 > 1$. Hence, we get:

$$\begin{aligned} \Pr(Z^z(m) \in B(S_{> r}^*)) &= \sum_{x \in S_{> r}^*} \mathcal{O}\left(\frac{1}{(\|x - z\| - 1)^3}\right) \\ &= \sum_{x \in S_{> r}^*} \mathcal{O}\left(\frac{1}{(\|x - x_z\| - 2)^3}\right) \\ &= \sum_{x \in S_{> r}^*} \mathcal{O}\left(\frac{1}{(\|\pi(x) - \pi(x_z)\| - 2)^3}\right) \\ &= \sum_{k \in \mathbb{Z}: k \geq r+2} \mathcal{O}\left(\frac{1}{k^2}\right) \\ &= \mathcal{O}\left(\frac{1}{r}\right). \end{aligned}$$

Where the third equality follows from the non-expansiveness of the projections. Therefore, by setting $r = m/\log m$, we get:

$$\Pr(Z^z(m) \in B(S^*)) = \mathcal{O}\left(\frac{\log m}{m}\right).$$

Hence, the numerator of Eq. 14 can be upper bounded as follows:

$$\sum_{m=0}^{m_0} \Pr(Z^z(m) \in B(S^*)) = 2 + \sum_{m=2}^{m_0} \mathcal{O}\left(\frac{\log m}{m}\right)$$

$$= \mathcal{O}(\log^2 n).$$

Altogether, combining the bounds for the numerator, those for the denominator, and Lemma 5.1 (with $m_0 = 2\sqrt[3]{n}$), we get the following result:

$$\mathbb{E}(m_{\text{detect}}^{X^{\text{cauchy}}}(S)) = \mathcal{O}\left(\frac{n \log^2 n}{\Delta_P}\right). \quad (18)$$

Finally, using Claim 2.1, we multiply this bound by the expected step-length $\tau = \mathcal{O}(\log n)$ to get the desired upper bound for the detection time, namely,

$$t_{\text{detect}}^{X^{\text{cauchy}}}(S) = \mathcal{O}\left(\frac{n \log^3 n}{\Delta_P}\right).$$

□

5.3 Proofs of technical Lemmas and Claims

5.3.1 Proof of Lemma 5.1

Since the proof of this lemma is the same as that of Lemma 19 in [Guinard and Korman \(2021\)](#), we omit it here.

5.3.2 Proof of Lemmas 5.2 and 5.3

Observation 5.5. *The probability to do a step of length at most $\ell > 0$ is $a\ell$ if $\ell \leq 1$ and $a(2 - \frac{1}{\ell})$ if $\ell > 1$. For integers $\ell_{\max} \geq \ell_2 \geq \ell_1 \geq 1$, the probability to choose a length in $[\ell_1, \ell_2]$ is $a(\frac{1}{\ell_1} - \frac{1}{\ell_2})$.*

The next claim quantifies the probability that the Cauchy process goes to a distance of at least d after m steps.

Claim 5.6. *For any integer $m \geq 2$ and any real $d \in [1, \frac{\ell_{\max}}{3}]$ we have,*

$$\Pr(\exists s \leq m \text{ s.t. } \|Z(s)\| \geq d) \geq 1 - e^{-cm/d},$$

for some constant $c > 0$. In particular this lower bound is at least

- $1 - O(m^{-3})$ if $d = c' \frac{m}{\log m}$ with $c' > 0$ a small enough constant,
- $\Omega(1)$ if $d = c'm$ for any constant $c' > 0$ with $c'm \leq \ell_{\max}/3$.

As the argument is identical to the proof of the analogous claim in the two-dimensional case (Claim 24 in the Supplementary Materials of [Guinard and Korman \(2021\)](#)), we omit it.

Claim 5.7. • *For any constant $c > 0$, there exists a constant $\delta > 0$ such that, for any two integers $1 \leq s \leq m$, we have $\Pr(\|Z(s)\| \leq cm) \geq \delta$.*

- *For any constant $0 < \delta < 1$, there exists a (large enough) constant $c > 0$ such that, for any two integers $1 \leq s \leq m$, we have $\Pr(\|Z(s)\| \leq cm) \geq \delta$.*

Proof Fix an integer $m \geq 1$ and let c'' be a constant to be specified later. Define \mathcal{A} as the event that each of the first m steps has length at most $\ell = c''m$. Then, for any integer $s \leq m$ and any constant $c > 0$, we have

$$\Pr(\|Z(s)\| \leq cm) \geq \Pr(\mathcal{A}) \cdot \Pr(\|Z(s)\| \leq cm \mid \mathcal{A}). \quad (19)$$

We now analyze each term appearing on the right-hand side of Eq. (19) individually and show that:

- For the first item of Claim 5.7, we choose $c'' > 0$ such that both factors become constants, so their product is bounded below by some constant δ .
- For the second item of Claim 5.7, where the bound δ is prescribed, we will show that both terms can be made at least $\sqrt{\delta}$ by choosing c and c'' appropriately.

Proceeding with the first term in the r.h.s of Eq. (19), by Observation 5.5, we have:

$$\Pr(\mathcal{A}) = \begin{cases} (ac''m)^m & \text{if } c''m \leq 1 \\ (2a)^m (1 - \frac{1}{2c''m})^m & \text{if } c''m \in [1, \ell_{max}] \\ 1 & \text{if } c''m \geq \ell_{max} \end{cases} .$$

For $1 \leq m \leq \frac{1}{c''}$, we have $(ac''m)^m \geq (ac''m)^{\frac{1}{c''}}$ as $ac''m \leq c''m \leq 1$, and $(ac''m)^{\frac{1}{c''}} \geq (ac'')^{\frac{1}{c''}}$ as $m \geq 1$. For the second item, note that the function $(1 - \frac{\alpha}{x})^x = e^{x \log(1 - \frac{\alpha}{x})}$ is increasing in $x \geq \alpha$ and thus, for $x \geq 2\alpha$, we have $(1 - \frac{\alpha}{x})^x \geq 2^{-2\alpha}$. Applying this with $\alpha = \frac{1}{2c''}$, we have, $(1 - \frac{1}{2c''m})^m \geq 2^{-\frac{1}{c''}}$, for $m \geq \frac{1}{c''}$. Overall, using $2a \geq 1$, we get

$$\Pr(\mathcal{A}) \geq \begin{cases} (\frac{c''}{2})^{\frac{1}{c''}} & \text{if } c''m \leq 1 \\ 2^{-\frac{1}{c''}} & \text{if } c''m \in [1, \ell_{max}] \\ 1 & \text{if } c''m \geq \ell_{max} \end{cases} .$$

Hence,

- $\Pr(\mathcal{A}) = \Omega(1)$ for any given $c'' > 0$.
- Moreover, for the second item of Claim 5.7, where $0 < \delta < 1$ is prescribed, we may choose c'' sufficiently large (in particular, $c'' \geq 1$, so that $c''m \geq 1$) to guarantee that $\Pr(\mathcal{A}) \geq 2^{-1/c''} \geq \sqrt{\delta}$.

We are now ready to lower bound the second factor in Eq. (19), namely $\Pr(\|Z(s)\| \leq cm \mid \mathcal{A})$. We introduce the following notation: for a random variable X , let $X^{\mathcal{A}}$ denote X conditioned on the event \mathcal{A} . Our first objective is to show that

$$\Pr(\|Z^{\mathcal{A}}(s)\| \leq cm) \geq 1 - \frac{16s \mathbb{E}(\|V^{\mathcal{B}}\|^2)}{c^2 m^2}, \quad (20)$$

where $V^{\mathcal{B}} = (V_1^{\mathcal{B}}, V_2^{\mathcal{B}}, V_3^{\mathcal{B}})$ is a one-step increment of the walk on \mathbb{R}^3 , conditioned on the event \mathcal{B} that its length is at most $c''m$.

Eq. (20) will be established by applying Chebyshev's inequality on each of the projections on the axes and using a union bound argument. Specifically, decomposing the walk Z on the three axes, by writing $Z = (Z_1, Z_2, Z_3)$, we first use a union bound to obtain:

$$\begin{aligned} \Pr(\|Z^{\mathcal{A}}(s)\| > cm) &\leq \Pr(\exists i = 1, 2, 3 \text{ s.t. } |Z_i^{\mathcal{A}}(s)| > cm/3) \\ &\leq \Pr(|Z_1^{\mathcal{A}}(s)| > cm/3) + \Pr(|Z_2^{\mathcal{A}}(s)| > cm/3) + \Pr(|Z_3^{\mathcal{A}}(s)| > cm/3) \\ &\leq 3 \Pr(|Z_1^{\mathcal{A}}(s)| > cm/3), \end{aligned}$$

where we used the symmetry to deduce that Z_1 , Z_2 , and Z_3 share the same distribution. Hence,

$$\Pr(\|Z^{\mathcal{A}}(s)\| \leq cm) \geq 1 - 3 \Pr(|Z_1^{\mathcal{A}}(s)| > cm/3).$$

Next, we aim to lower bound the right-hand side. Using that $\mathbb{E}[Z_1^{\mathcal{A}}(s)] = 0$ for all s , Chebyshev's inequality yields:

$$\Pr(|Z_1^{\mathcal{A}}(s)| > cm/3) \leq \frac{9 \text{Var}(Z_1^{\mathcal{A}}(s))}{c^2 m^2}.$$

Since $Z_1^{\mathcal{A}}(s)$ is the sum of s independent steps that follow the same law as $V_1^{\mathcal{B}}$, we have:

$$\text{Var}(Z_1^{\mathcal{A}}(s)) = s \text{Var}(V_1^{\mathcal{B}}).$$

As the expectation of $V_1^{\mathcal{B}}$ is zero, we have $\text{Var}(V_1^{\mathcal{B}}) = \mathbb{E}((V_1^{\mathcal{B}})^2)$. Furthermore, since $|V_1^{\mathcal{B}}| \leq \|V^{\mathcal{B}}\|$, we obtain:

$$\text{Var}(Z_1^{\mathcal{A}}(s)) \leq s \mathbb{E}(\|V^{\mathcal{B}}\|^2),$$

which concludes the proof of Eq. (20). Next, we estimate $\mathbb{E}(\|V^{\mathcal{B}}\|^2)$. If $c''m \leq 1$, then under the conditioning on \mathcal{A} , the step length is chosen uniformly at random from $[0, c''m]$. Thus, its second moment is

$$\mathbb{E}(\|V^{\mathcal{B}}\|^2) = \int_0^{c''m} \ell^2 \frac{d\ell}{c''m} = \frac{(c''m)^2}{3}. \quad (21)$$

On the other hand, if $c''m \geq 1$, then $V^{\mathcal{B}}$ is a Cauchy walk with cut off $\ell_{max} = c''m$. Hence, its second moment is

$$\mathbb{E}(\|V^{\mathcal{B}}\|^2) = a' \int_0^1 \ell^2 d\ell + a' \int_1^{c''m} \ell^2 \ell^{-2} d\ell \quad (22)$$

$$\leq a' \int_0^{c''m} 1 d\ell = a' c''m \leq c''m. \quad (23)$$

Overall, by Eqs. (20), (21) and (23) we find that, for $s \leq m$,

$$\begin{aligned} \Pr(\|Z^{\mathcal{A}}(s)\| \leq cm) &\geq \begin{cases} 1 - \frac{27sc''m^2}{3c^2} & \text{if } c''m \leq 1 \\ 1 - \frac{27sc''}{c^2m} & \text{if } c''m \geq 1 \end{cases} \\ &\geq \begin{cases} 1 - \frac{27c''}{3c^2} & \text{if } c''m \leq 1 \\ 1 - \frac{27c''}{c^2} & \text{if } c''m \geq 1 \end{cases}. \end{aligned}$$

We then conclude the proof of Claim 5.7 by observing the following.

- For the first item of Claim 5.7, we have proved that $\Pr(\mathcal{A}) = \Omega(1)$ for any constant $c'' > 0$. Hence, we may now choose c'' small enough so that $\Pr(\|Z^{\mathcal{A}}(s)\| \leq cm) = \Omega(1)$.
- For the second item of Claim 5.7, we have already chosen c'' to be large (in order to have $\Pr(\mathcal{A}) \geq \sqrt{\delta}$), but we are free to choose c large enough so that $\Pr(\|Z^{\mathcal{A}}(s)\| \leq cm) \geq \sqrt{\delta}$.

□

To conclude, we give the proofs of Lemmas 5.2 and 5.3.

Proof of Lemma 5.2

Given the claims established above, the proof of Lemma 5.2 follows the same steps as the proof of Lemma 20 in [Guinard and Korman \(2021\)](#). Therefore, we omit it.

Proof of Lemma 5.3

Let $\alpha > 0$ and $m \in [2, \alpha \ell_{max}]$. By the monotonicity property stated in Corollary 2.3, it suffices to prove the result for $x = 0$. Indeed, for any $x \in \mathbb{R}^3$, the sets $B(0) \setminus B(x)$ and $B(x) \setminus B(0)$ have the same volume A and

$$\begin{aligned} \Pr(Z(m) \in B(x) \setminus B(0)) &\leq A \max_{y \in B(x) \setminus B(0)} \{p^{\|Z(m)\|}(y)\} \\ &\leq A \min_{y \in B(0) \setminus B(x)} \{p^{\|Z(m)\|}(y)\} \\ &\leq \Pr(Z(m) \in B(0) \setminus B(x)), \end{aligned}$$

where the second inequality relies on the monotonicity property together with the observation that any point in $B(x) \setminus B(0)$ is more than unit distance from the origin, and thus farther from 0 than every point in $B(0) \setminus B(x)$. This shows that $\Pr(Z(m) \in B(x)) \leq \Pr(Z(m) \in B(0))$, hence it is sufficient to prove the required upper bound for $x = 0$. Intuitively, we argue that with high probability there is some step $s \leq m$ at which $Z(s)$ becomes “distant” (at least $cm/\log m$ away). Once this is conditioned on, the probability of being in $B(0)$ at step m is small, thanks to the monotonicity property (Corollary 2.3). Formally, consider a (small) positive constant c , and let \mathcal{A} be the event that there is some $s \leq m$ for which $\|Z(s)\| \geq cm/\log m$. Consider $B(0)$ the ball of radius 1 with center 0. Write

$$\begin{aligned} \Pr(Z(m) \in B(0)) &= \Pr(Z(m) \in B(0) \cap \mathcal{A}) + \Pr(Z(m) \in B(0) \cap \neg\mathcal{A}) \\ &\leq \Pr(Z(m) \in B(0) \mid \mathcal{A}) + \Pr(\neg\mathcal{A}), \end{aligned} \tag{24}$$

By the first item of Claim 5.6, taking c to be sufficiently small, we have

$$\Pr(\neg\mathcal{A}) = O(m^{-3}).$$

To rewrite the remaining term in Eq. (24), we introduce the notation Z^x for the Cauchy process on \mathbb{R}^3 with cutoff ℓ_{max} starting from $Z(0) = x$. Because our process starts at 0, we have $Z = Z^0$. Observe further that Z^x has the same distribution as Z^0 translated by x . Using this notation, we obtain the next bound, with the second inequality following from the Markov property:

$$\begin{aligned} \Pr(Z^0(m) \in B(0) \mid \mathcal{A}) &\leq \max_{s \leq m} \Pr(Z^0(m) \in B(0) \mid \|Z^0(s)\| \geq cm/\log m) \\ &\leq \max_{s \leq m} \sup_{\|x\| \geq cm/\log m} \Pr(Z^x(m-s) \in B(0)) \end{aligned}$$

$$\begin{aligned}
&= \max_{s \leq m} \sup_{\|x\| \geq cm/\log m} \Pr(Z^x(s) \in B(0)) \\
&= \max_{s \leq m} \sup_{\|x\| \geq cm/\log m} \Pr(Z^0(s) \in B(-x)) \\
&= \max_{s \leq m} \sup_{\|x\| \geq cm/\log m} \Pr(Z(s) \in B(x))
\end{aligned}$$

Use now Corollary 2.3 that gives $p^{Z(m)}(x) \leq \frac{3}{4\pi\|x\|^3}$. Hence, for any $x \in \mathbb{R}^3$ with $\|x\| > 1$, we have

$$\Pr(Z(m) \in B(x)) = \int_{B(x)} p^{Z(m)}(y) dy \leq \int_{B(x)} \frac{3}{4\pi(\|x\| - 1)^3} dy = \frac{1}{(\|x\| - 1)^3}.$$

Let $m(c)$ be the largest integer $m > 0$ such that $cm/\log m \leq 2$. For $m > m(c)$, we have

$$\Pr(Z(s) \in B(x)) \leq \max_{s \leq m} \frac{1}{(cm \log m - 1)^3} = \frac{1}{(cm \log m - 1)^3}$$

Overall, we find that, for $m > m(c)$

$$\Pr(Z(m) \in B(0)) \leq \frac{1}{(cm/\log m - 1)^3} + \frac{c'}{m^3},$$

which we can bound by $\frac{c_2 \log^3 m}{m^3}$ for some constant $c_2 > 0$. Since $m(c)$ is a constant, there is some other constant $c_3 > 0$ for which, for any $m \in [2, m(c)]$, we have $\Pr(Z(m) \in B(0)) \leq \frac{c_3 \log^3 m}{m^3}$. We then obtain, for any $m \geq 2$,

$$\Pr(Z(m) \in B(0)) \leq \frac{\max\{c_2, c_3\} \log^3 m}{m^3},$$

which concludes the proof.

6 Approximately convex targets

In this section, we introduce the class of *approximately convex* targets and show that (1) the Cauchy walk is almost optimal for this class and (2) it contains all convex targets.

Definition 6.1. *A compact target S is approximately convex if*

$$\frac{\Delta_P}{\Delta_B} \geq \frac{1}{36}.$$

Observe that (1) this ratio is always at most 1 by definition, and (2) if the condition holds, it remains valid upon scaling the target by any factor $r > 0$. Moreover, the class of valid targets grows larger as the right-hand side constant decreases. Although this

constant could be relaxed further, the remainder of this section establishes that its current value already captures a broad class of targets. Moreover, Section 6.3 presents a counterexample of a target that is not approximately convex, valid for any constant.

6.1 Optimality of the Cauchy walk

In this section, we demonstrate that for approximately convex targets, the Cauchy walk achieves optimal performance up to polylogarithmic factors. To show this, we first note that, by the definition of approximate convexity, both the universal lower bound (Theorem 3.1) and the upper bound for $\mu = 2$ (Theorem 5.4) can be equivalently expressed in terms of either parameter — up to constant factors. Consequently, the Cauchy walk identifies approximately convex targets in nearly optimal time, regardless of whether Δ_B or Δ_P serves as the governing parameter. In particular, the expected detection time differs from the universal lower bound by at most a polylogarithmic factor of $\mathcal{O}(\log^3 n)$.

6.2 Convex targets are approximately convex

This subsection demonstrates that convex targets are inherently approximately convex. Recall that we always assume that targets are piecewise smooth sets with well-defined surface area and projected surface area.

Theorem 6.2. *Every convex target is approximately convex.*

Proof Consider a convex target S of surface area Δ . To establish Theorem 6.2, It suffices to show that

$$\frac{\Delta}{\Delta_B} \geq \frac{1}{6}, \quad \frac{\Delta}{\Delta_P} \leq 6,$$

Where Δ , Δ_B , and Δ_P denote the surface area, face surface area, and largest projection area of S , respectively.

Lemma 6.3. $\frac{\Delta}{\Delta_B} \geq \frac{1}{6}$.

Proof Let $x, y \in S$ be the points that maximize $\|x - y\|$ then the diameter of S is defined as $D_1 := \|x - y\|$. (For simplicity, we assume compactness of S and therefore such x and y exist; otherwise, we can take x and y , whose distance from each other is arbitrarily close to the diameter of S). This is realized along some unit vector $u_1 = (x - y) / \|x - y\|$. Next, let D_2 be the diameter of the projection of S in the orthogonal plane u_1^\perp and let u_2 be its corresponding unit vector (in the direction of the vector realizing of D_2). Consider a bounding box B' of S whose largest face Q' is parallel to the plane spanned by u_1 and u_2 . Let $\mathbf{Area}(\pi_{Q'}(S))$ denote the area of the projection of S onto Q' . Since S is convex, its projection onto Q' is a planar convex set containing two orthogonal lines of length D_1 and D_2 , and therefore its area is $\mathbf{Area}(\pi_{Q'}(S)) \geq \frac{1}{2}D_1D_2$. Next, observe that since Q' is the largest face of the bounding box B' , we have:

$$\Delta_{B'} = \mathbf{Area}(Q') = D_1D_2.$$

Combining the two bounds yields

$$\text{Area}(\pi_{Q'}(S)) \geq \frac{1}{2} \Delta_{B'}.$$

Finally, since $\text{Area}(\pi_{Q'}(S))$ is the area of a projection of S , the surface area of S satisfies

$$\Delta \geq \text{Area}(\pi_{Q'}(S)),$$

hence $\Delta \geq \frac{1}{2} \Delta_{B'}$. Observe that, by the definition, Δ_B is the largest face area of the smallest bounding box and for any target we have $\Delta_{B'} \geq \frac{1}{3} \Delta_B$. Consequently, $\Delta \geq \frac{1}{6} \Delta_B$, which completes the proof. \square

Lemma 6.4. $\frac{\Delta}{\Delta_P} \leq 6$.

Proof Recall that we assume that the boundary ∂S of S is piecewise smooth. Let $u \in \mathbb{R}^3$ be a unit vector, and let π_{u^\perp} denote the orthogonal projection onto the plane orthogonal to u .

Then the area of the orthogonal projection of S onto u^\perp is given by

$$\text{Area}(\pi_{u^\perp}(S)) = \frac{1}{2} \int_{\partial S} |n(x)^\top u| dA(x),$$

where $n(x)$ denotes the unit vector that is orthogonal to the surface ∂S at x , and $dA(x)$ is the surface area element on ∂S (See Vouk (1948) for a reference). By definition, Δ_P is areas of the largest projection of S onto the six faces of its bounding box B . Since the box is composed of three pairs of parallel faces aligned with an orthonormal basis $\{e_1, e_2, e_3\}$, we have:

$$\Delta_P \geq \frac{1}{3} \sum_{i=1}^3 \text{Area}(\pi_{e_i^\perp}(S)) = \frac{1}{6} \int_{\partial S} \sum_{i=1}^3 |n(x)^\top e_i| dA(x),$$

Note that $\sum_i |n(x)^\top e_i|$ is the L_1 norm of the unit normal $n(x)$. Given that $1 \leq \|n(x)\|_1 \leq \sqrt{3}$ for any unit vector in \mathbb{R}^3 , integrating these bounds over the surface ∂S yields $\Delta_P \geq \Delta/6$, which concludes the proof. \square

Finally, combining Lemmas 6.3 and 6.4 with the definition of approximate convexity completes the proof of Theorem 6.2. \square

6.3 Supporting evidence for Δ_P as a main parameter governing detection time

We have seen that for (approximately) convex targets, the parameters Δ , Δ_B , and Δ_P are all proportional, making the universal lower bound and the upper bound for the Cauchy strategy compatible. To further understand which parameter could best represent the running time, we next illustrate that both Δ and Δ_B could not be used in the formula in Theorem 5.4 instead of Δ_P .

- **Surface area Δ .** Consider a construction parameterized by an integer r : define a connected target S that fits within a large ball of radius r , and consists of $\Theta(r^3)$ disjoint balls of constant radius. This target has total surface area $\Theta(r^3)$, and if Theorem 5.4 were to apply with this parameter, its detection time would be $\mathcal{O}\left(\frac{n \log^3 n}{r^3}\right)$. However, detecting this target necessarily entails detecting the

bounding box $\text{Box}(S)$, which has surface area $\Theta(r^2)$ and requires at least $\Omega(\frac{n}{r^2})$ time, by the universal lower bound. When $r \gg \log^3 n$, this leads to a contradiction, implying that in Theorem 5.4, the parameter Δ_P cannot be directly replaced with the surface area Δ of a general target.

- **Bounded surface area Δ_B .** Consider a target S consisting of two orthogonal line segments of length L and unit thickness. Define the inflated target as $S^{(r)} = \{rx \text{ with } x \in S\}$, then the surface area of the inflated target scales as $\sim r^2 L$, implying that the maximal projection area satisfies $\Delta_P^{(r)} \approx cr^2 L$. In contrast, the surface area of the bounding box scales as $\Delta_B^{(r)} \approx c' r^2 L^2$. Consequently,

$$\frac{\Delta_P^{(r)}}{\Delta_B^{(r)}} \sim \frac{1}{L}.$$

Therefore, for sufficiently large L , this ratio falls below $1/12$, and the target fails to be approximately convex.

7 Diffusive Lévy walks searching a line target

7.1 Lévy walks on the discrete torus

In this section, we consider a discrete 3D torus \mathbb{T} containing n nodes, and a target S that is a path of length L parallel to one of the axes. Recall that the searcher starts at a node chosen uniformly at random, hence, we may assume without loss of generality that S lies on the x -axis. The searcher moves over this graph according to a Lévy walk X of parameter μ following the general construction of Clementi et al. (2021); a precise definition of this process is provided in Methods, Section 2. We let $t_{\text{detect}}^X(S)$ represent the expected time until the search process X finds the target S for the first time.

The goal of this section is to prove the following:

Theorem 7.1. *Let X be a Lévy walk with parameter $\mu > 2$ on the discrete three-dimensional cubic torus graph with n nodes and let the target S be a path of length L parallel to one of the axes. Then,*

$$\mathbb{E}[t_{\text{detect}}^X(S)] = \mathcal{O}\left(\frac{n \log n}{L}\right).$$

It's reasonable to assume that X is a lazy random walk, where at each step, the probability of staying in the same position is $1/2$. Indeed, if we show that the lazy version of the process detects the target in time $\mathcal{O}\left(\frac{n \log n}{L}\right)$, the detection time for the non-lazy version will also be bounded by the same time.

7.2 Upper bounds on hitting (and mixing) times of Lévy walks

To prove the theorem, we first establish upper bounds on the hitting and mixing steps for a Lévy walk with $\mu > 2$ on either the discrete 1D cycle or the 2D torus. While such bounds have been qualitatively noted in the literature (e.g. Chiarini et al. (2021)), we were unable to find a formal proof; we therefore provide a rigorous derivation below. Specifically, we prove that these values are bounded from above by the corresponding hitting and mixing steps of a simple random walk.

Theorem 7.2. *A Lévy walk with parameter $\mu > 1$ starting from a fixed node on a one-dimensional cycle with m nodes has expected hitting step $\mathcal{O}(m^2)$, whereas on a two-dimensional torus with m^2 nodes its expected hitting step is $\mathcal{O}(m^2 \log m)$.*

The proof of this theorem is derived from several structural properties of the Lévy walk on either the cycle or the two-dimensional torus. We categorize all processes satisfying these conditions as isotropic walks.

Definition 7.3. *We say that a Markov chain on a torus of any dimension is an isotropic walk if it satisfies the following properties:*

1. *The process is transitive, meaning that the behavior of the walk looks the same from any starting point.*
2. *The process is symmetric, i.e., the probability of moving from u to v is the same as moving from v to u .*
3. *The probability of transition from any node to an adjacent neighbor (at distance 1) is a constant $0 < c \leq 1$ invariant with respect to the chosen specific neighbor.*

Theorem 7.2 follows from Theorem 7.4 below, by applying on it the Lévy walk on the two-dimensional torus and on the cycle, since both are isotropic walks. Indeed, the first two conditions of Definition 7.3 hold by construction, while the third is satisfied because the constant c is at least one-quarter the probability of a unit-length step. This probability, given by the normalization constant $\left(\sum_{l=1}^{l_{\max}} l^{-\mu}\right)^{-1}$, remains lower-bounded by a constant for all $\mu > 1$.

Theorem 7.4. *An isotropic walk starting from a fixed node on a one-dimensional cycle with m nodes has expected hitting step $\mathcal{O}(m^2)$, whereas on a two-dimensional torus with m^2 nodes its expected hitting step is $\mathcal{O}(m^2 \log m)$.*

Proof We show that the expected hitting step of an isotropic walk is bounded above (up to constants) by the expected hitting time of the simple random walk on the one or two dimensional discrete torus, respectively. Since the latter is known to satisfy the claimed upper bounds (e.g., Levin and Peres (2017)), the same bounds follow for isotropic walks.

Hitting step on the two-dimensional torus

We can interpret the isotropic walk on the two-dimensional torus as a random walk on a complete weighted graph. Here, the edges represent all possible transitions, with weights

assigned according to the corresponding transition probabilities of the original walk. Denote this graph G and observe that it is transitive and undirected due to the definition of isotropic walk, hence the expected hitting time between node a and b is given by the product between the number of nodes in the graph and the effective resistance between those two nodes (this follows from Proposition 10.10 and Proposition 10.7 in [Levin and Peres \(2017\)](#)). In symbols,

$$\mathbb{E}_a[m_{\text{hit}}(b)] = \frac{m^2}{2} \mathcal{R}^G(a \leftrightarrow b). \quad (25)$$

where $\mathbb{E}_a[m_{\text{hit}}(b)]$ denotes the expected hitting step of node b when the process starts from node a , and m^2 is the total number of nodes in the two-dimensional torus. Observe that, by Rayleigh's Monotonicity Law (Corollary 9.13 in [Levin and Peres \(2017\)](#)), deleting edges from G cannot decrease the effective resistance. Hence, letting G' be the graph obtained from G by removing all edges but those between neighboring nodes on the two-dimensional torus, the right-hand side of Eq. (25) is at most $\frac{m^2}{2} \mathcal{R}^{G'}(a \leftrightarrow b)$. By isotropy, every edge of G' has the same weight $0 < c \leq 1$, rescaling all edge weights by a factor $1/c$ yields the graph $c^{-1}G'$, i.e., G' with all edge weights equal to 1; this graph is exactly the two-dimensional discrete torus and note that its effective resistance $\mathcal{R}^{c^{-1}G'}(a \leftrightarrow b)$ is $c\mathcal{R}^{G'}(a \leftrightarrow b)$. Under this rescaling, the expected hitting step is upper bounded by $\frac{m^2}{2c} \mathcal{R}^{c^{-1}G'}(a \leftrightarrow b)$. But is lower bounded by a constant and the hitting step of the simple walk on the two dimensional torus is $2m^2 \mathcal{R}^{c^{-1}G'}(a \leftrightarrow b)$ (See Eq. (10.27) in [Levin and Peres \(2017\)](#)), so we have that

$$\mathbb{E}_a[m_{\text{hit}}(b)] = \mathcal{O}\left(\mathbb{E}_{a^c}^{G'}[m_{\text{hit}}(b)]\right) = \mathcal{O}\left(m^2 \log m\right),$$

where $\mathbb{E}_{a^c}^{G'}[m_{\text{hit}}(b)]$ denotes the expected hitting step of the node b for the simple random walk on the two-dimensional torus, started from a ; and the second equality follows from Proposition 10.21 in [Levin and Peres \(2017\)](#).

Hitting step on the cycle

We proceed exactly as in the two-dimensional case; the only difference is that we now start from isotropic walk on the cycle and we build the corresponding auxiliary graphs from its one-step transitions. Let C be the weighted graph formed from a cycle in which each node is connected to every other node. For each pair of nodes, we assign to the their edge the weight given by the one-step probability that the walk moves between them. Since the process is symmetric, this weight is the same in both directions, so C is an undirected weighted graph. Now define C' from C by deleting all edges except those joining nearest neighbors on the cycle (i.e., nodes at distance 1 on the cycle graph). By translation invariance, C' is a cycle in which every remaining edge has the same weight $0 < c \leq 1$. If we rescale all edge weights by the factor c^{-1} , the resulting walk coincides with the simple random walk on the cycle. It is well known that for the simple random walk on a cycle with m nodes, the maximal expected hitting step is $\mathcal{O}(m^2)$ (see Example 10.27 in [Levin and Peres \(2017\)](#) for a formal proof).

This completes the proof of Theorem 7.4. \square

7.3 Proof of Theorem 7.1

Following the same steps as in the proof of Claim 2.1, one sees that the claim also applies in the discrete setting, where τ denotes the expected step length with respect to the Manhattan distance. For $\mu > 2$, this expectation is $\mathcal{O}(1)$ (see Fact 1.1). Therefore,

to prove Theorem 7.1, it suffices to prove:

$$\max_a \mathbb{E}_a [m_{\text{hit}}^X(S)] = \mathcal{O}\left(\frac{n \log n}{L}\right), \quad (26)$$

where $\mathbb{E}_a[\cdot]$ denotes the expected value when X starts from node a . Indeed,

$$\mathbb{E} [m_{\text{hit}}^X(S)] = \mathbb{E}_\pi [m_{\text{hit}}^X(S)] \leq \max_a \mathbb{E}_a [m_{\text{hit}}^X(S_{yz})],$$

where $\mathbb{E}_\pi[\cdot]$ denotes expectation under the uniform initial distribution π , and the first equality follows from the assumption that the initial node is chosen uniformly at random.

We are interested in the projections of the 3D walk X on both the x -axis, and on the yz -plane. In particular, let $m_{\text{mix}}^{(x)}(\cdot)$ be the mixing step of the 1D random walk X_x and $m_{\text{hit}}^{(yz)}(\cdot)$ be the hitting step of the 2D random walk X_{yz} .

Theorem 7.5. *Let X be an irreducible and aperiodic Markov chain on the three-dimensional cubic torus with n nodes. Assume that X satisfies the following:*

- X has uniform stationary distribution,
- $m_{\text{mix}}^{(x)}(1/n^2) = \mathcal{O}\left(\mathbb{E}\left[m_{\text{hit}}^{(yz)}(S_{yz})\right]\right)$, and
- $\mathbb{E}_a\left[m_{\text{hit}}^{(yz)}(S_{yz})\right] = \mathcal{O}(n^{2/3} \log n)$ for every a on the yz -plane.

Then

$$\max_a \mathbb{E}_a [m_{\text{hit}}^X(S)] = \mathcal{O}\left(\frac{n \log n}{L}\right).$$

Proof Let T be a positive integer to be defined later and set $\tau_0 := 0$. For $i \geq 1$, let τ_i be the first step after $\tau_{i-1} + T$ steps, at which the projected walk X_{yz} visits the projected target set S_{yz} . Formally,

$$\tau_i := \inf\{m \geq \tau_{i-1} + T : X_{yz}(m) \in S_{yz}\}.$$

Likewise, let J be the smallest $i \geq 1$ such that $X(\tau_i) \in S$, i.e., the smallest index at which the 3D walk hits S . Since the detection step is the first m with $X(m) \in S$, we have the bound

$$m_{\text{hit}}^X(S) \leq \tau_J.$$

that holds for every starting node. Moreover, by telescoping,

$$\tau_J = \sum_{i=1}^J (\tau_i - \tau_{i-1}) = \sum_{i=1}^{\infty} (\tau_i - \tau_{i-1}) \mathbf{1}_{\{J \geq i\}}.$$

Taking expectations with respect to a fixed starting node $X(0) = a$,

$$\mathbb{E}_a [m_{\text{hit}}^X(S)] \leq \sum_{i=1}^{\infty} \mathbb{E}_a \left[(\tau_i - \tau_{i-1}) \mathbf{1}_{\{J \geq i\}} \right]. \quad (27)$$

For each i , apply the tower property with respect to $X(0), X(1), \dots, X(\tau_{i-1} + T)$, i.e., the initial position $X(0)$, together with the first $\tau_{i-1} + T$ steps:

$$\mathbb{E}_a \left[(\tau_i - \tau_{i-1}) \mathbf{1}_{\{J \geq i\}} \right] = \mathbb{E}_a \left[\mathbf{1}_{\{J \geq i\}} \mathbb{E}[\tau_i - \tau_{i-1} \mid X(0), \dots, X(\tau_{i-1} + T)] \right], \quad (28)$$

where the equality holds because $\mathbf{1}_{\{J \geq i\}}$ is a function of $X(0), \dots, X(\tau_{i-1} + T)$.

Claim 7.6. $\mathbb{E}_a[m_{\text{hit}}^X(S)] \leq \left(T + \mathcal{O}\left(n^{2/3} \log n\right)\right) \mathbb{E}_a[J]$.

Proof Let $\mathbb{E}_a\left[m_{\text{hit}}^{(yz)}(S_{yz})\right]$ be the expected value of $m_{\text{hit}}^{(yz)}(S_{yz})$ when a is the initial location of the searcher in the projected chain. Observe that after the deterministic waiting steps of T steps after τ_{i-1} (and before τ_i), the additional expected steps required to hit S_{yz} depends only on the projected process started from position $X_{yz}(\tau_{i-1} + T)$. Hence, the inner conditional expectation in Eq. (28) can be rewritten as

$$\mathbb{E}[\tau_i - \tau_{i-1} \mid X(0), \dots, X(\tau_{i-1} + T)] = T + \mathbb{E}_{X_{yz}(\tau_{i-1} + T)}\left[m_{\text{hit}}^{(yz)}(S_{yz})\right].$$

By assumption, the expected hitting step is upper bounded by $\mathcal{O}\left(n^{2/3} \log n\right)$, which is independent of i . Thus, we can rewrite Eq. (28) as follows

$$\mathbb{E}_a\left[(\tau_i - \tau_{i-1})\mathbf{1}_{\{J \geq i\}}\right] = \left(T + \mathcal{O}\left(n^{2/3} \log n\right)\right) \mathbb{E}_a\left[\mathbf{1}_{\{J \geq i\}}\right]. \quad (29)$$

Substituting Eq. (29) in Eq. (27), we obtain

$$\begin{aligned} \mathbb{E}_a[m_{\text{hit}}^X(S)] &\leq \left(T + \mathcal{O}\left(n^{2/3} \log n\right)\right) \sum_{i \geq 1} \mathbb{E}_a\left[\mathbf{1}_{\{J \geq i\}}\right] \\ &= \left(T + \mathcal{O}\left(n^{2/3} \log n\right)\right) \mathbb{E}_a[J]. \end{aligned} \quad (30)$$

This completes the proof of the claim. \square

Claim 7.7. $\mathbb{E}_a[J] = \Theta\left(\frac{n^{1/3}}{L}\right)$

Proof By assumption, the mixing step of the process projected onto the x -axis is $m_{\text{mix}}^{(x)}(1/n^2) \leq Cn^{2/3} \log n$ for some positive constant C and n large enough. Hence, after $m_{\text{mix}}^{(x)}(1/n^2)$ steps the distribution of the process on the x -axis is approximately uniform. In particular, the probability that X_x is on a node w is

$$\left[\frac{1}{n^{1/3}} - \frac{1}{n^2}, \frac{1}{n^{1/3}} + \frac{1}{n^2}\right],$$

Moreover, for every $m \geq m_{\text{mix}}^{(x)}(1/n^2)$ and for all u and w lying on the x -axis:

$$\mathbb{P}(X_x(\tau_{i-1} + m) = w \mid X_x(\tau_{i-1}) = u) = \Theta\left(\frac{1}{n^{1/3}}\right).$$

Thus, if we set

$$T = Cn^{2/3} \log n,$$

then $X_x(\tau_i)$ is almost uniform on the x -axis, regardless of its location at step τ_{i-1} . Formally, since $T \geq m_{\text{mix}}^{(x)}(1/n^2)$ and $\tau_i - \tau_{i-1} \geq T$, we obtain that for every v and u on the x -axis:

$$\mathbb{P}(X_x(\tau_i) = v \mid X_x(\tau_{i-1}) = u) = \Theta\left(\frac{1}{n^{1/3}}\right). \quad (31)$$

Observe that Eq. (31) implies that if we know the starting point and that $X_x(\tau_{i-1})$ did not hit the target, then the probability of hitting it at step τ_i is $\Theta(L/n^{1/3})$. That is,

$$\begin{aligned}
& \mathbb{P}\left(X_x(\tau_i) \in S_x \left| \bigcap_{j=1}^{i-1} X_x(\tau_j) \notin S_x, X(0) = a \right.\right) \\
&= \sum_u \mathbb{P}(X_x(\tau_i) \in S_x \mid X_x(\tau_{i-1}) = u) \mathbb{P}\left(X_x(\tau_{i-1}) = u \left| \bigcap_{j=1}^{i-1} X_x(\tau_j) \notin S_x, X(0) = a \right.\right) \\
&= \Theta\left(\frac{L}{n^{1/3}}\right) \sum_u \mathbb{P}\left(X_x(\tau_{i-1}) = u \left| \bigcap_{j=1}^{i-1} X_x(\tau_j) \notin S_x, X(0) = a \right.\right) \\
&= \Theta\left(\frac{L}{n^{1/3}}\right),
\end{aligned}$$

where the second equality follows from the fact that S_x has cardinality L together with Eq. (31), while the third equality holds because the sum is taken over all possible events and therefore equals 1.

Finally, we can prove that the expected value of J is $\mathcal{O}(n^{1/3}/L)$. In symbols,

$$\begin{aligned}
\mathbb{P}(J \geq k \mid X(0) = a) &= \mathbb{P}\left(\bigcap_{i=1}^{k-1} X_x(\tau_i) \notin S_x \mid X(0) = a\right) \\
&= \prod_{i=1}^{k-1} \mathbb{P}\left(X_x(\tau_i) \notin S_x \left| \bigcap_{j=1}^{i-1} X_x(\tau_j) \notin S_x, X(0) = a \right.\right) \\
&= \prod_{i=1}^{k-1} \left[1 - \mathbb{P}\left(X_x(\tau_i) \in S_x \left| \bigcap_{j=1}^{i-1} X_x(\tau_j) \notin S_x, X(0) = a \right.\right)\right] \\
&= \prod_{i=1}^{k-1} \left[1 - \Theta\left(\frac{L}{n^{1/3}}\right)\right] \\
&= \left[1 - \Theta\left(\frac{L}{n^{1/3}}\right)\right]^{k-1}.
\end{aligned}$$

Consequently, J has a geometric tail, and hence $\mathbb{E}_a[J] = \Theta\left(\frac{n^{1/3}}{L}\right)$. \square

Altogether, substituting this bound and the definition of T into Eq. (30) yields $\mathbb{E}_a \left[m_{\text{hit}}^X(S) \right] = \mathcal{O}\left(\frac{n \log n}{L}\right)$. This completes the proof of Theorem 7.5. \square

Observe that the Lévy walk on the three-dimensional torus is irreducible and aperiodic, and admits the uniform distribution as its stationary measure (X satisfies Eq. (1.29) in Levin and Peres (2017)). Therefore, it suffices to show that $m_{\text{mix}}^{(x)}(1/n^2)$ and $\max_a \mathbb{E}_a \left[m_{\text{hit}}^{(yz)}(S_{yz}) \right]$ are both $\mathcal{O}(n^{2/3} \log n)$ in order to apply Theorem 7.5 to the Lévy walk.

Lemma 7.8. *X_x has expected hitting step $\mathcal{O}(n^{2/3})$ and X_{yz} has expected hitting step $\mathcal{O}(n^{2/3} \log n)$ for every starting node.*

Lemma 7.8 follows from the observation that X_x and X_{yz} are isotropic walks on a cycle with $n^{1/3}$ nodes and a two-dimensional torus with $n^{2/3}$ nodes, respectively. Hence, the bounds on the hitting steps follow by applying Theorem 7.4 to the projected Lévy walks. Finally, we can use the hitting step on the cycle to upper bound $m_{\text{mix}}^{(x)}(1/n^2)$, the *mixing step*, i.e., the minimum number of steps needed for the total variation distance to the stationary distribution to drop below $1/n^2$.

Lemma 7.9. *The mixing step along the x -line is $m_{\text{mix}}^{(x)}(1/n^2) = \mathcal{O}(n^{2/3} \log n)$.*

Proof By construction, the chain X_x has a probability of at least $1/2$ of remaining at its current state at each step. Recall that we defined $m_{\text{mix}}^{(x)} := m_{\text{mix}}^{(x)}(1/4)$; consequently, applying Theorem 10.22 in Levin and Peres (2017), the mixing step of the projected chain X_x satisfies

$$m_{\text{mix}}^{(x)} \leq 2M_{\text{hit}}^{(x)} + 1, \quad M_{\text{hit}}^{(x)} := \max_{a,b} \mathbb{E}_a \left[m_{\text{hit}}^{(x)}(b) \right],$$

where $\mathbb{E}_a[\cdot]$ denotes expectation for the chain started from a , and $m_{\text{hit}}^{(x)}(b)$ is the hitting step of node b for X_x . From Theorem 7.8, one obtains that $M_{\text{hit}}^{(x)}$ is $\mathcal{O}(n^{2/3})$, and therefore $m_{\text{mix}}^{(x)} = \mathcal{O}(n^{2/3})$. Finally, by the standard amplification bound for total variation mixing steps,

$$m_{\text{mix}}^{(x)}(\varepsilon) = \mathcal{O} \left(m_{\text{mix}}^{(x)} \log \frac{1}{\varepsilon} \right) = \mathcal{O} \left(n^{2/3} \log \frac{1}{\varepsilon} \right).$$

In particular, setting $\varepsilon = 1/n^2$ gives

$$m_{\text{mix}}^{(x)}(1/n^2) = \mathcal{O}(n^{2/3} \log n).$$

□

Altogether, Lemmas 7.9 and 7.8 enable us to apply Theorem 7.5 to the Lévy walk on the torus, thereby completing the proof of Eq. (26), thus completing the proof of Theorem 7.1.

References

- Ariel G, Rabani A, Benisty S, et al (2015) Swarming bacteria migrate by lévy walk. Nature communications 6(1):8396
- Bartumeus F, Peters F, Pueyo S, et al (2003) Helical lévy walks: adjusting searching statistics to resource availability in microzooplankton. Proceedings of the National Academy of Sciences 100(22):12771–12775
- Bénichou O, Loverdo C, Moreau M, et al (2011) Intermittent search strategies. Reviews of Modern Physics 83(1):81–129
- Boyer D, Ramos-Fernández G, Miramontes O, et al (2006) Scale-free foraging by primates emerges from their interaction with a complex environment. Proceedings of the Royal Society B: Biological Sciences 273(1595):1743–1750

- Chiarini L, Jara M, Ruszel WM (2021) Constructing fractional gaussian fields from long-range divisible sandpiles on the torus. *Stochastic Processes and their Applications* 140:147–182
- Clementi A, d’Amore F, Giakkoupis G, et al (2021) Search via parallel levy walks on \mathbb{Z}^2 . In: *Proceedings of the 2021 ACM Symposium on Principles of Distributed Computing*, pp 81–91
- Guinard B, Korman A (2021) Intermittent inverse-square lévy walks are optimal for finding targets of all sizes. *Science advances* 7(15):eabe8211
- Harris TH, Banigan EJ, Christian DA, et al (2012) Generalized lévy walks and the role of chemokines in migration of effector cd8+ t cells. *Nature* 486(7404):545–548
- Humphries NE, Queiroz N, Dyer JR, et al (2010) Environmental context explains lévy and brownian movement patterns of marine predators. *Nature* 465(7301):1066–1069
- de Jager M, Weissing FJ, Herman PM, et al (2011) Lévy walks evolve through interaction between movement and environmental complexity. *Science* 332(6037):1551–1553
- James A, Plank MJ, Edwards AM (2011) Assessing lévy walks as models of animal foraging. *Journal of the Royal Society Interface* 8(62):1233–1247
- Levernier N, Textor J, Bénichou O, et al (2020) Inverse square lévy walks are not optimal search strategies for $d \geq 2$. *Physical review letters* 124(8):080601
- Levin DA, Peres Y (2017) *Markov chains and mixing times*, vol 107. American Mathematical Soc.
- Raichlen DA, Wood BM, Gordon AD, et al (2014) Evidence of lévy walk foraging patterns in human hunter–gatherers. *Proceedings of the National Academy of Sciences* 111(2):728–733
- Reynolds AM, Frye MA (2007) Free-flight odor tracking in drosophila is consistent with an optimal intermittent scale-free search. *PloS one* 2(4):e354
- Reynolds AM, Smith AD, Menzel R, et al (2007) Displaced honey bees perform optimal scale-free search flights. *Ecology* 88(8):1955–1961
- Rhee I, Shin M, Hong S, et al (2011) On the levy-walk nature of human mobility. *IEEE/ACM transactions on networking* 19(3):630–643
- Shlesinger MF, Klafter J (1986) Lévy walks versus lévy flights. In: *On growth and form: Fractal and non-fractal patterns in physics*. Springer, p 279–283
- Sims DW, Southall EJ, Humphries NE, et al (2008) Scaling laws of marine predator search behaviour. *Nature* 451(7182):1098–1102

- Vershynin R (2018) High-dimensional probability: An introduction with applications in data science, vol 47. Cambridge university press
- Viswanathan GM, Buldyrev SV, Havlin S, et al (1999) Optimizing the success of random searches. *nature* 401(6756):911–914
- Viswanathan GM, Raposo E, Da Luz M (2008) Lévy flights and superdiffusion in the context of biological encounters and random searches. *Physics of Life Reviews* 5(3):133–150
- Vouk V (1948) Projected area of convex bodies. *Nature* 162(4113):330–331